Author(s): Hakonen, Maria & Piitulainen, Harri & Visala, Arto

Title: Current state of digital signal processing in myoelectric interfaces and related applications

Year: 2015

Version: Final published version

Please cite the original version:

Hakonen, Maria & Piitulainen, Harri & Visala, Arto. 2015. Current state of digital signal processing in myoelectric interfaces and related applications. Biomedical Signal Processing and Control. P. 334-359. 1746-8094 (printed). DOI: 10.1016/j.bspc.2015.02.009

Biomedical Signal Processing and Control 18 (2015) 334–359

Contents lists available at ScienceDirect

Biomedical Signal Processing and Control

journal homepage: www.elsevier.com/locate/bspc

Review

Current state of digital signal processing in myoelectric interfaces and related applications

Maria Hakonen[a,c,*], Harri Piitulainen[b,1], Arto Visala[a,2]

[a] Department of Electrical Engineering and Automation, School of Electrical Engineering, Aalto University, PO Box 15500, 00076 Aalto, Finland
[b] Brain Research Unit, Department of Neuroscience and Biomedical Engineering, 15100, 00076 Aalto, Espoo, Finland
[c] Brain and Mind laboratory, Department of Neuroscience and Biomedical Engineering, School of Science, Aalto University, PO Box 15100, 00076 Aalto, Espoo, Finland

ARTICLE INFO

Article history:
Received 18 July 2014
Received in revised form
27 December 2014
Accepted 11 February 2015

Keywords:
Surface electromyography
Myoelectric interface
Classification
Feature extraction
Pattern recognition

ABSTRACT

This review discusses the critical issues and recommended practices from the perspective of myoelectric interfaces. The major benefits and challenges of myoelectric interfaces are evaluated. The article aims to fill gaps left by previous reviews and identify avenues for future research. Recommendations are given, for example, for electrode placement, sampling rate, segmentation, and classifiers. Four groups of applications where myoelectric interfaces have been adopted are identified: assistive technology, rehabilitation technology, input devices, and silent speech interfaces. The state-of-the-art applications in each of these groups are presented.

Contents

* Corresponding author at: Department of Electrical Engineering and Automation, School of Electrical Engineering, Aalto University, PO Box 15500, 00076 Aalto, Finland. Tel.: +358 50 3823008.
E-mail addresses: maria.hakonen@aalto.fi (M. Hakonen), harri.piitulainen@aalto.fi (H. Piitulainen), arto.visala@aalto.fi (A. Visala).
[1] Tel.: +358 50 568 0654.
[2] Tel.: +358 50 5755936.

http://dx.doi.org/10.1016/j.bspc.2015.02.009

1. Introduction

The wearable and mobile technology market has demonstrated significant growth and adoption in various end-user market segments, in particular telecommunication, fitness, wellness, healthcare, and medical monitoring. However, the technology lacks an effective method to communicate with devices. Currently popular input methods such as touch screens, small keyboards, and portable controllers are impractical in situations where hands cannot easily be used to directly manipulate an input device. Portable input devices are also difficult to carry around. Additionally, for people with severe physical disabilities such as spinal cord injury, quadriplegia, hemiplegia, Parkinson's disease, or muscular dystrophy, the traditional user interfaces currently available are inadequate. Fehr et al. [1] surveyed 200 practicing clinicians, asking them to provide information about their patients with power wheelchairs relying on conventional controllers. Of respondents, 85% reported evaluating some number of patients annually for whom a power wheelchair is not an option because they cannot control it. Of the patients, 40% with power wheelchairs had difficulties with steering tasks and 5–9% needed assistance with such tasks. Such examples indicate the need for new controller interfaces accommodating the abilities of the patients. Attempts have been made to overcome these problems by using voice commands [2], as well as camera- [3], electroencephalography (EEG)- [4], electrooculography (EOC)- [5] or electromyography (EMG)-based control [6].

EMG interface classifies the voluntary-contraction-related muscle activity and associates it to the desired function of the given device. The EMG interface could offer an intuitive and easy way of communication that relieves the user from portable control devices and direct eye contact to the device. The only requirement is that the user is able to activate some of his or her voluntary skeletal muscles. EMG interfaces generate control commands for a given device relying on information content of EMG signals. The methods used to measure these signals include surface EMG (sEMG) where electrodes are placed on the skin over the measured muscle, intramuscular EMG (iEMG) where the electrodes are inserted through the skin into the muscle tissue and percutaneous EMG (pEMG) where a needle or wire is inserted under the skin and subcutaneous tissue over the aponeurosis of the muscle. According to our best knowledge, pEMG measurements have not been used in the EMG interfaces. Comparative studies have found that, at least in laboratory conditions, intramuscular and surface recordings yield similar accuracy in classifying hand and forearm movements [7,8]. Surface electrodes are advantageous because they are inexpensive and noninvasive. In contrast to relatively selective intramuscular electrodes, surface electrodes detect activity from many muscles on one channel, which makes it possible to acquire sufficient information for the EMG interface with smaller number of electrodes [8]. However, intramuscular recordings may be beneficial because of their potential ability to overcome some of the major problems of surface recordings, such as electrode shifts and skin impedance changes. Because iEMG [7–13] and have seldom been investigated in the context of EMG interfaces, this study deals only with sEMG recordings.

The sEMG signal is a superposition of individual motor unit action potentials (MUAPs) within the pick-up range of the surface electrodes. As sEMG amplitude and frequency content changes with contraction-force level [14,15], it is possible to associate the muscle contractions of the user to control the device concerned. The concept of sEMG interface was introduced in the 1940s [16], and the first sEMG application, a myoelectric prosthetic arm, was developed in 1960 [17]. In the recent years, the interest has grown toward sEMG interfaces. It has been noted that myoelectric interfaces have a huge potential in applications designed not only for people with disabilities [18–24] but also in applications for healthy people [25–30]. The numerous benefits of the sEMG interface over traditional input devices have inspired patents [31,32], especially in the field of mobile technology.

The sEMG interface is suggested to offer many benefits over other man–machine control methods. The sEMG control may require less attention from the user than EEG based controls or the control with eye movements. In contrast to visual-based control, myoelectric control allows the user to look around while controlling the device. Compared to many other biosignals, such as EEG, sEMG signals have relatively high signal-to-noise ratio. Unlike voice control, sEMG control has only a minimal delay, is not sensitive to ambient sound perturbations, does not cause embarrassment to the user, or disrupt the environment. The sEMG interfaces can

offer an alternative interface that require only minimal motor skills from the user, which is a significant improvement for people with impaired motor skills. However, to get accustomed with the interface, some training is always required. The electrodes can be left under the clothes or even be imbedded into them [33,34]. Some textile electrodes, *e.g.* "smart shorts" measuring EMG activity (Mbody, Myonteck Ltd., Kuopio, Finland), are commercially available. Their control commands can be given by subtle motions or different levels of static (isometric) muscle contractions. Therefore, the sEMG interface does not mark the user as handicapped or in need of special concessions.

sEMG signals can be measured from the superficial muscles of the body [35]. Muscles of the upper limbs [18,36], the lower limbs [37], the shoulder or the head, face, and neck [38–40] have been applied in the sEMG interfaces. Thus, a person with mobility disabilities can control the device with the muscle(s) that he/she is still able to contract. For example, a person with quadriplegia can control the device with contractions of facial muscles [19], and it is possible to record the sEMG signal from the amputee's stump skin to command the prosthesis [18,36,41,42]. This allows an intuitive control because it allows the amputee to command for example a grasp posture of prosthesis simply by performing the corresponding action with his/her residual muscles.

This article aims to discuss and conclude the most important issues related to sEMG signal measurement and processing from sEMG interface point of view as well as give a review of the state-of-art applications for sEMG control. Related reviews have been previously published by Oskoei and Hu [43], Miscera et al. [21] and Merletti et al. [44]. This review is organized as follows. First, the themes related to the acquisition system are discussed, including optimal electrode type and configuration, sampling, filters, and preprocessing algorithms. Second, the steps in decoding of sEMG commands are studied. Based on recent literature, recommendations are suggested for segmentation strategy, feature selection and the type of classifier. The final chapter introduces applications with sEMG interface.

2. Acquisition system

The objective of the acquisition system and signal processing is to provide a high quality sEMG signal(s) where the posture or muscle contraction specific information can be extracted and associated with the desired control command using classifiers, proportional or threshold algorithms, onset analysis, or finite state machines. The acquisition electronics of the sEMG interface consists of sEMG channels, filters, amplifiers, and an A/D converter. This section concentrates on the most essential issues in the design of an acquisition system: sEMG electrodes, cut-off frequencies of filters, sampling rate, and preprocessing algorithms.

2.1. sEMG electrodes

In sEMG interfaces, voluntary-contraction-related muscle activity is detected when the user contracts his/her muscles in order to control a device. The sEMG signal is composed of superpositioned motor unit action potentials propagating underneath the electrode(s) along the active muscle fibers (along their excitable membrane—the sarcolemma) starting from innervation zones (*i.e.* neuromuscular junctions) toward the tendon regions [45]. The electrodes measuring the sEMG signal form an sEMG channel.

The most common electrode derivations used in sEMG interfaces include bipolar, monopolar, and Laplacian configuration. Typically, one channel bipolar derivation is applied, in which sEMG signal is the voltage difference between a pair of recording surface electrodes aligned along the length of the skin surface of the muscle [46]. Monopolar electrode configuration measures a difference between the electrode on active site (the muscle) and a common reference electrode on non-active site (typically on bony area) [47]. Laplacian configuration uses typically one central surface electrode and number of surrounding electrodes, and has also recently shown promise in sEMG interfaces [48,49]. Research interest has also increased toward high-density sEMG (HD-sEMG) where a dense grid of surface electrodes allowing various electrode derivations is placed on a restricted skin area [50,51].

This subsection aims to give recommendations for electrode type, size and inter-electrode distance, as well as the placement and number of electrodes in the context of sEMG interfaces. These issues are important in regard to classification accuracy, computational time and production costs of the sEMG control system. More detailed recommendations for sEMG measurements can be found for example from the website of the Surface ElectroMyoGraphy for the Non-Invasive Assessment of Muscles (SEMIAM) project [35,52], but they are not necessarily always optimal for customized sEMG interfaces. A review by Merletti et al. [46] discusses more deeply the sEMG electrode system and amplifier technology.

2.1.1. Electrode types

sEMG signals can be measured both with wet and dry electrodes. Commonly used wet electrodes require conductive electrolyte gel or sponge between the electrode and the skin, but can provide high quality sEMG signals. The wet electrodes often require skin preparation (*e.g.* shaving and skin abrasion), which can reduce skin–electrode impedance and motion artifacts [53]. However, the preparation is somewhat time consuming and requires expertise. In addition, the wet electrodes may not be optimal for long-term use in sEMG interfaces since the conductive gel may dry, can cause irritation and discomfort, and is potential cause of skin allergy and inflammation [54]. Modern dry electrodes do not require conductive gel and skin preparation, and still can reach signal quality comparable to wet electrodes [55]. For this reason, the dry electrodes may be more applicable for sEMG interfaces [46].

The material of the electrode affects its electrochemical behavior [56]. Polarizable electrodes (*e.g.* gold, platinum and iridium electrodes) are characterized by capacitive behavior because only displacement current passes between the skin and electrode whereas non-poralizable electrodes (*e.g.* galvanized and sintered Ag/AgCl electrodes) behave like resistors since they allow a free flow of charge across the electrode–skin interface [56]. No electrode is perfectly non-polarizable or polarizable but approximates these characteristics. Polarizable electrodes are not recommended for sEMG measurements because of their high sensitivity to motion artifacts [46,56]. Commonly used non-polarizable silver–silver chloride (Ag/AgCl) electrodes are highly stabile. The Ag/AgCl electrodes consist of a silver metal surface plated with a thin layer of silver chloride [53,54]. Some polymers and fabric of threads coated by a conductive layer have also both shown promise as an electrode materials. Such dry electrodes are ideally suited for textile integration, and can yield sEMG signal quality comparable to wet Ag/AgCl electrodes [57].

2.1.2. Size and shape of electrodes

To our best knowledge, Young et al. [58] are the only authors who considered an optimal electrode size for sEMG interfaces. Their study is made with bipolar in the context of pattern recognition-based control strategy that decides the control commands on the basis of the posture-specific values of feature vectors calculated from multiple EMG signals. The electrode sizes (1 cm × 1 cm, 2 cm × 2 cm and 3 cm × 3 cm) were shown not to significantly affect classification accuracy and completion rates in target achievement control [58]. However, the benefit of large electrodes was that the sEMG signals acquired with them were significantly less sensitive

to the changes of sEMG recording site when shifted up to 2 cm in perpendicular to the muscle fibers [58]. This was because the electrode with the largest pickup volume was possibly recording a portion of the same source as in the non-shifted condition. An alternative strategy suggested to reduce the effect of electrode shifts on classification accuracy is to include exemplars of possible shifts in the training session of the classifier [59,60]. However, this approach is time consuming and troublesome because the electrodes have to be moved to expected displacement locations during the training of the classifier.

No recommendations for the sEMG-electrode shape for sEMG interfaces were found in the literature, and in many studies the shape of the electrodes was not reported. Also SENIAM has not found clear and objective criteria for a recommendation for electrode shape and expected no major influence on the sEMG signal from taking different electrode shapes [61]. However, there is evidence that particular electrode types may be associated with spectral dips in the sEMG power spectrum [62]. Typically, circular, rectangular or bar electrodes are used in the sEMG interfaces. In special situations, such as when determining mean spectral frequency of sEMG signal or estimating mean muscle fiber conduction velocity, transversal (with respect to longitudinal axis of the muscle fibers) bar electrodes may be more appropriate than electrodes with larger longitudinal dimension, *e.g.*, square electrodes [63].

2.1.3. Inter-electrode distance

Bipolar EMG channels are preferred in sEMG interfaces as they are more tolerant to noise than for example monopolar ones. The larger the inter-electrode distance (IED) is, *i.e.* the distance between the two electrode poles that form a bipolar channel, the wider the pick-up volume sampled and the higher but less spatially specific the amplitude of the signal. A rough estimate of an electrode distance volume is a sphere with radius equal to the IED [64]. Most studies of sEMG interfaces have followed the recommendation of SENIAM and used an IED of 20 mm, which yields relatively selective recordings. The optimal IED also depends on the distance between the recording electrodes and the source muscle. Based on modeled sEMG signals, sEMG amplitude is reduced less in superficial muscles than in the deeper ones if IED is reduced from typical 20 mm to 10 mm [63]. Nevertheless, the sEMG signal is always dominated by superficial sources, *i.e.* MUAPs, closest to (typically within 10–20 mm) the electrode [23]. Young et al. [64] found that IEDs larger than commonly recommended 20 mm were consistently more tolerant against electrode shifts and thus recommended the use of IEDs of up to 40 mm. Although larger IED increases the likelihood of crosstalk from nearby muscles, the benefit is a smaller electrode shift relative to the electrode detection volume [23]. A potential configuration for sEMG interfaces could be a spatially selective concentric-ring electrode reducing both the effect of electrode shift and crosstalk [65].

IED also is critical to HD-sEMG systems. The sampling rate in space is related to IED, and too long IED may result the sampling of surface potentials at the rate below Nyqvist frequency, and thus generating spatial aliasing. A recent study [66] demonstrated that in order to avoid spatial aliasing maximum IED of 10 mm should be used, and recommended the IEDs to be below 10 mm for HD-sEMG systems.

2.1.4. Placement of electrodes

The signal-to-noise ratio of sEMG signals can be improved by placing the electrodes as close to the sEMG signal source as possible. The electrodes are separated from the muscle of interest by a layered volume conductor composed of subcutaneous tissue (adipose tissue and other soft tissues), and the skin, acting as a spatial low-pass filter smoothing the detected MUAPs and thus decreasing their amplitude and frequency content [46]. Thus, both amplitude and frequency content of the sEMG signal are affected by the distance between the sEMG electrodes and the sources.

It is recommended that bipolar sEMG channels should be placed on the propagating part of the muscle, between the endplate area, *i.e.* innervation zone (IZ), and tendon region. In fusiform muscles, the IZ is typically a relatively narrow band from where the MUAPs propagate bidirectionally toward the tendons [67]. However, pennate muscles with a more complicated structure, including many upper-limb muscles, have more complex and diffusively localized IZs [67]. Especially, if bipolar sEMG electrodes are placed on opposite sides of the IZ, there may occur a substantial level of cancelation of the physiological sEMG signal, reducing its amplitude [68]. Thus, a small displacement of the sEMG electrodes with respect to the IZ may substantially reduce the amplitude of the bipolar sEMG signal, and especially its low-frequency components [68]. To get accurate and repeatable measurements, the IZs should be identified on subject-by-subject basis, using an electrode array [69]. Although, the distribution of IZs has been reported for several human muscles [67,69,70], general distributions of IZs are not necessarily valid for all individuals because of a large variability in the location of major IZs within and between subjects [70]. Additionally, a shift in IZs can occur with dynamic changes in joint angle [71] and even in static conditions when isometric contraction level is increased [72]. Muscle undergoes substantial three-dimensional changes in its geometry, especially during dynamic contractions, and thus sEMG electrodes are shifted with respect to the underlying muscle fibers and IZs [73]. Due to these issues, it is not possible to totally avoid the effect of IZs, but their effects should be optimally minimized.

In most studies of sEMG interfaces, common recommendations are followed, and the bipolar electrodes are placed parallel to muscle fibers. However, this placement is very sensitive to electrode shifts that may occur in real use of sEMG interfaces [59]. There have been studies on untraditional electrode orientation where a channel oriented perpendicularly with respect to muscle fibers is formed by calculating differential between an electrode from one control site and the corresponding electrode from the control site on the opposite side of the arm [58,64,74]. Although, these transverse channels yield poorer classification accuracy than traditional bipolar channels placed longitudinally with respect to muscle fibers, using transverse channels in addition to traditional channels has proved to be useful for ensuring low classification error with and without electrode shift [64]. This result is achieved by comparing the electrode configurations with the same number of channels. The benefit of using transverse channels is that they provide global information (muscle group), useful especially when electrode shifts are present, while solely longitudinal channels result relatively selective (muscle-specific) recordings. Transverse and longitudinal channels are illustrated in Fig. 1.

Another possible approach to reduce the effect of IZs and electrode shifts would be use of HD-sEMG that has shown promise in the sEMG based control in the last years [34,50,51,75,76]. As HD-sEMG "scans" almost the whole muscle skin surface it is less sensitive to issue of electrode locations and re-placements compared to one channel bipolar configuration. In addition, HD-sEMG provides extraction of features from EMGs that depend on the spatial distribution of the MUAPs in the same muscle, and on the load-sharing between muscles if the electrode grid extents over several muscles. This may aid in differentiation between tasks and effort levels. The effect of IZs may also be reduced using HD-sEMG in which the IZ channels can be detected and thus be discarded from the analyses [77].

In studies on pattern recognition-based sEMG interfaces, bipolar electrodes have been placed either with reference to specific muscles or equidistantly over the muscles of interest. The untargeted approach would be more preferable in sEMG interfaces because

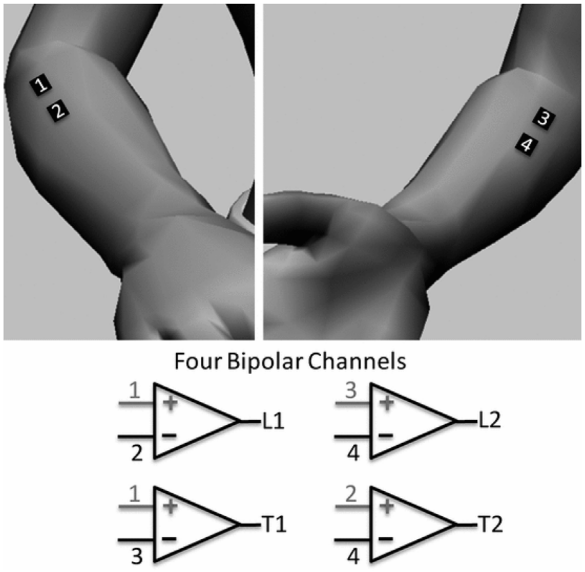

Fig. 1. Longitudinally (channels L1 and L2) and transversely (T1 and T2) oriented electrodes.

it is simpler to implement. The targeting of specific muscles may increase classification accuracy [8], but not always [7]. Comparisons of intramuscular and surface electrodes have shown that local intramuscular measurements do not outweigh the relatively global surface recordings in sEMG classification [7,8]. It seems that when amplitude information is available from most of the muscles involved in motion, the classifier is capable to yield high classification accuracy. More important than the initial placement of electrodes is that the information content of the measurements is consistent during the use of the sEMG interface and training session. Thus, the sEMG classification system should be robust against displacements of electrodes.

2.1.5. Number of electrodes

The optimal number of electrodes for sEMG interfaces has mostly been studied by placing the electrodes on the forearm [7,8,64,78,79]. In laboratory conditions, the increase in classification accuracy has become saturated with three to four bipolar channels [7,8]. A relatively small number of electrodes have been shown to be sufficient also when electrode shifts are present: the recommended subset is four to six bipolar channels, of which one half were longitudinal channels and the other half transverse channels [64]. However, the optimal number of electrodes may also depend on individual anatomy of the subject. Andrews et al. [78,79] increased the number of bipolar channels from one to eight, and for four subjects the classification accuracy remained very poor until increased sharply when the number of channels was five or seven. For eight subjects, the classification accuracy increased significantly up to three electrodes. The classification was tested during a typing task with the classification system optimized individually for each subject.

When incrementally adding new channels, the channels that gave the best classification accuracy for small subsets were relatively far from each other, as would be expected because they provide most new information to the classifier [7,8,78]. Where gross hand and forearm postures have been studied, the optimal electrode subset usually includes electrodes placed approximately on *flexor digitorum superficials*, *flexor capri ulnaris*, *extensor capri radialis longus* or *brevis*, and *extensor capri ulnaris* [7,8], whereas when studying finger movements, the selected electrodes were placed approximately on *flexor digitorum prefunds* and *extensor digitorum communis* [78,79].

The drawback of small number of electrodes is that the fault of only one electrode can cause significant degradation in classification accuracy. The malfunctioning channels (*e.g.* due to bad skin–electrode contact) can be automatically detected and removed [80], but re-training of the classifier is still needed. HD-sEMG relying on spatial-domain information (*e.g.* experimental variogram) could solve this problem since HD-sEMG has shown to be capable to maintain high performance even without re-training when some electrodes are omitted [76]. The drawbacks of HD-sEMG based systems are increased production costs and computational demands. However, the drop in performance has shown to be relatively small when the number of electrodes used in the training of the classifier is reduced from 96 to 24 [76]. The development of more powerful microprocessors enables the use of HD-sEMG. Moreover, it has been shown that e-textiles can be used in HD-sEMG systems, and thus are easy to apply, are non-obtrusive and allow a classification accuracy of ~90% for nine hand and wrist postures [34].

2.2. Filtering and sampling rate

The amplitude of sEMG signal is typically well below 10 mV, which makes it sensitive to artifacts. Therefore, it is amplified typically 100–5000-fold with amplifier, preferably as close to the recording electrodes as possible, and filtered prior to an A/D conversion. High-pass cut-off ranging between 5 and 20 Hz is typically used in sEMG studies to eliminate slow signal variations caused mainly by artifact motion due to the movement of electrodes and their cables and typically ranging between 0 and 20 Hz. However, Li et al. [81,82] suggest a high-pass cut-off at 60 Hz for sEMG interfaces because the lower frequency components of sEMG spectrum mainly contain information on firing rates of active motor units, which may not make a significant contribution to the movement classification [61]. They found that sEMG power between 20–100 Hz only slightly improves the classification accuracy for healthy subjects (by 0.25%) and transradial amputees (by 1.6%). The use of a high-pass filter at 60 Hz more than effectively attenuates the motion artifacts as well as power interferences by alternating current (at the frequency of 50 Hz in Europe).

The dominant energy (about 95%) of an sEMG signal is limited to harmonics up to 400–500 Hz, *i.e.* the components over 500 Hz can be considered as noise [83]. According to the Nyqvist rule, to avoid aliasing, the sampling rate should be equal to twice the highest frequency of interest contained within the signal. Therefore, the sampling the rate of 1000 Hz with a low-pass filter at 400–450 Hz is commonly used in sEMG recordings. However, sampling rates lower than 1000 Hz may still preserve sufficient physiological information for accurate classification of the movements. One benefit of the lower sampling rate is simultaneously reduced processing and computational complexity for the controller of the sEMG interface. Li et al. [81,82] found that sampling at 500 Hz could be computationally more optimal than typical 1000 Hz for sEMG interfaces, as the respective classification accuracy was decreased only by 0.8% in healthy subjects and by 2.2% in amputees but halved both the storing memory and data processing time [81]. To avoid aliasing, the sampling rate of 500 Hz requires a low-pass filter with cut-off frequency below 250 Hz.

2.3. Preprocessing algorithms for classification

The algorithms used to preprocess sEMG data for classification include classwise principal component analysis (cPCA) and independent component analysis (ICA). In cPCA, sEMG data are rotated by class-specific projection matrixes to spatially decorrelate the

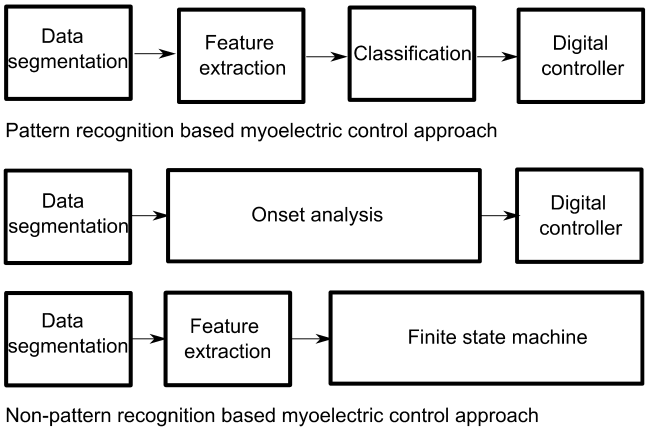

Fig. 2. Schematic diagrams of pattern and non-pattern recognition-based sEMG control methods.
© [2007] IEEE. Adapted with permission, from Ref. [43].

data before features are extracted [84]. The projection matrixes approximate some nonlinear low-dimensional data manifold. This in a way tunes the data, allowing the classifier to identify the motion classes better. Hargrove et al. [85] found that, by using cPCA, the analysis window length can be cut from 256 ms to 128 ms without affecting the classification accuracy. Their other study [86] showed that, when cPCA is used, classification errors reduced significantly for both intact-limbed and amputee subjects.

ICA can be used to reduce the crosstalk effect in sEMG interfaces. ICA estimates the set of independent sEMG signals from a mixture of given signals by estimating an un-mixing matrix [87]. Ganesh et al. [88] compared the performance of different ICA algorithms for isometric hand gesture identification using four channel sEMG. Temporal Decorrelation Source Separation (TDSEP) yielded the best performance of 1 s duration for an analysis window. Al-Timemy et al. [89] found that the FastICA preprocessing technique increases classification accuracy for different window lengths from 88% to 93%. The sEMG data has been shown to be super Gaussian at low contraction levels [90], which matches the FastICA assumption about non-gaussianity.

3. Decoding myoelectric information

sEMG control strategies can be separated into two main groups: pattern recognition-based and non-pattern recognition-based strategies [21,43]. The phases required to decode motor commands in the two systems are illustrated in Fig. 2.

Pattern recognition-based approaches calculate feature vectors from segments of the signal and use them as an input to a classifier for the prediction of postures. Non-pattern-based methods include proportional, onset analysis, and finite state machines. Unlike pattern recognition-based methods, they do not allow one-to-one mapping, but their advantages are simple implementation and no need of training. Next sections describe each stage required to decode muscle contractions to the device control commands. The stages are data segmentation, feature extraction, feature reduction, as well as pattern recognition- and non-pattern recognition-based classification.

3.1. Segmentation

In sEMG interfaces, the sEMG data needs to be analyzed in real-time. Therefore, the analysis is performed on time segments, namely windows, epochs or segments. This section discusses the three issues, *i.e.* windowing technique, segment length and the state of EMG signal, that need to be considered in segmentation. These parameters affect both the classification accuracy and response time of the system.

3.1.1. Windowing technique

There are two alternative windowing techniques: adjacent windowing and overlapped windowing [43,91,92]. In the former technique, custom-length consecutive segments are used for analysis and feature extraction. Because of high-speed processors, the processing time is usually less than the duration of time segment, which makes the processor idle for a certain amount of time, as can be seen in Fig. 3 (left). Overlapped windowing uses the idle time for acquiring more data to be processed. As Fig. 3 (right) illustrates, each segment overlaps the previous one. The overlapped window approach is more appropriate in sEMG control systems because it produces better classification accuracy and a more constant controller delay and reduces the length of the maximum delay [92]. With large segments, overlapped windowing is necessary in order to avoid long latency in real time operation [93].

3.1.2. Segment length

Large data windows increase classification accuracy, but the drawback is that more time is required to collect and process larger data sets. Thus, a trade-off has to be done between classification accuracy and real-time constrains. The effect of classification errors and time delay on controllability has mostly been investigated in the context of upper limb prostheses [58,91,94,95] but is essential in all real-time applications. A test where the user moved a virtual limb to one of six predetermined target positions showed that classification errors less than ~10% yield controllable systems whereas classification errors over ~35% yield systems that are not controllable [58]. Estimates of the delay (*i.e.* the time between onsets of user's command and actuation of the device) which does not make the prosthesis feel unresponsiveness to the user range between 50 ms and 400 ms [91,92,95–99]. This delay range corresponds to window lengths of 50–400 samples and 25–200 samples for sampling frequencies of 1000 Hz and 500 Hz, respectively.

In theory, a segment of $t \leq 200$ ms contains enough information to estimate motion states of a limb because that is the minimum interval between distinct contractions [93]. However, high classification accuracy is also possible with segments less than 200 ms if the features have been selected carefully and if majority voting (MV) is used as a postprocessing mechanism, as can be seen in Figs. 4 and 5. In sEMG signal processing, MV is a common postprocessing technique that aims to increase the overall classification accuracy by analyzing the current class decision along with the $n-1$ previous class decisions [92]. As is apparent from Fig. 4, the accuracy of the unprocessed decision stream degrades rapidly by decreasing segment length, but MV effectively prevents degradation with the help of more decisions available with short segments. It should be noticed that MV also increases the delay because the more votes is used the more windows need to be processed before the final decision. No appreciable difference exists in classification accuracy whether a large window with small number of votes or a small window with a large number of votes is used [91]. However, short windows are recommended because they need less storage space. The saving in storage space is important when implementing the classifier as an embedded system where memory is usually a scare resource [92]. When MV is used with overlapped segmentation, no great improvement on performance is apparent, but there is a notable decrease in the discrepancy of accuracy over different sessions [93]. The optimal window length also depends on the feature vector calculated from windows in pattern recognition-based classification [93], as shown in Fig. 5. A more detailed description of the features is given in Section 3.2.

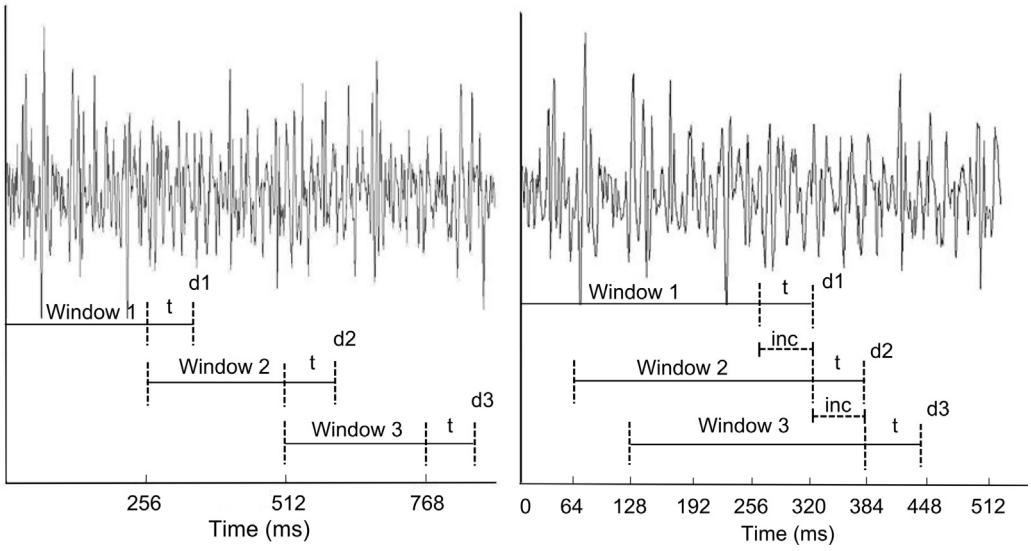

Fig. 3. Windowing techniques. Each analysis window takes finite time to process (t) before a decision (d1, d2, d3) can be produced. In adjacent windowing (left), the classifier is idle majority of time because the processing time is much less than window length. Overlapped windows (right) increase frequency of class decisions because analysis window slides along at relatively small increments (inc). Setting the amount of overlap equal to the processing time allows the controller to begin processing next class decision immediately when the previous decision has been completed.

Figure is modified version from Ref. [91], available: http://www.rehab.research.va.gov/jour/11/486/pdf/farrell486.pdf.

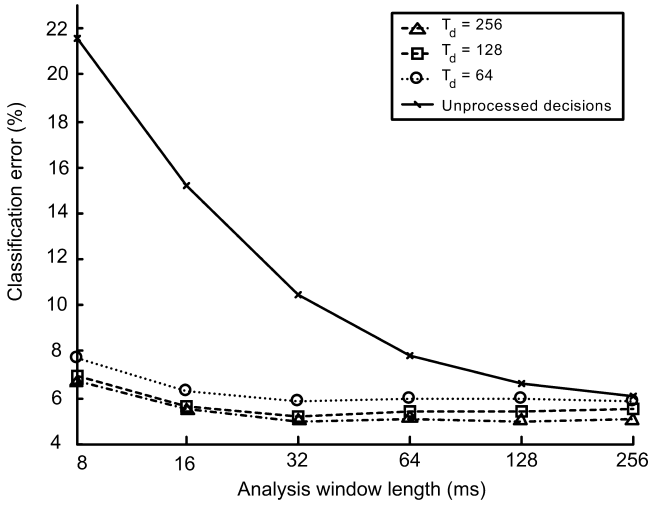

Fig. 4. Classification error *vs.* window length. T_d = delay due to MV.
© [2003] IEEE. Reprinted, with permission, from Ref. [92].

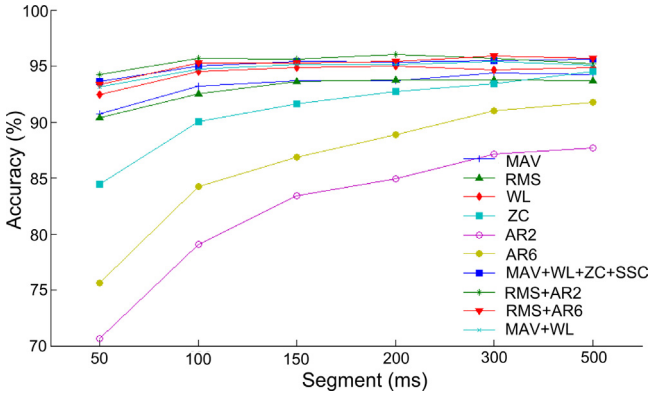

Fig. 5. Classification accuracy for some single features and feature vectors. Overlapped segmentation with an increment of 200 ms was applied for segment lengths of 300 ms and 500 ms while disjoint segmentation was applied for the other segment sizes. MAV = mean absolute value; RMS = root mean square; WL = waveform length; ZC = zero crossing; AR2 = 2nd order autoregressive coefficients; AR6 = 6th order autoregressive coefficients.
© [2008] IEEE. Reprinted, with permission, from Ref. [93].

3.1.3. State of the sEMG signal

The sEMG classification studies have usually considered two alternative states of sEMG signal: a transient state and a steady state [95,100]. The transient state emanates from burst of simultaneous motor unit activity, as a muscle goes from rest to some voluntary contraction level or when the contraction force is dynamically deviated from a steady contraction level. In the steady state, a muscle is under a constant (isometric) contraction. It has been shown that the features extracted during isometric contraction can be classified more accurately than the features extracted during dynamic contraction [100], and therefore most studies have used steady-state signals to generate the training data [86,93,103]. In addition, the data recorded during isometric contraction allows faster system response because the degradation of classification accuracy is not as profound when the window length is decreased. The main drawback of using transient sEMG signals is that it prohibits switching from class to class in an effective or intuitive manner because a contraction must initiate from rest [95]. This severely impedes the coordination of complex tasks involving multiple degrees of freedoms (DOFs). When steady-state data is used, an sEMG signal is in undetermined state during transition between different levels of contractions. Therefore, the classification errors that occur when switching between classes should be reduced by using majority voting. However, an approach to classify both transient and steady-state signals concurrently has shown to outperform the methods that investigate these two states separately [8,104]. Including some dynamic portions of sEMG signal during the learning process significantly improved the performance of both a linear discriminant analysis (LDA) [8,104] classifier and a support vector machine (SVM) classifier compared to the static training [104].

In addition, muscle fatigued and non-fatigued states can be distinguished [101,102]. EMG signal varies over time due to number of reasons, *e.g.*, motor learning, muscle fatigue, and post-activity potentiation. The muscle fatigue has been defined as inability to maintain given task demands [101,102], and can be of both central

and peripheral origin [101,102]. Muscle fatigue can develop within a few seconds or a few minutes depending on the task [105]. Muscle fatigue alters the task or posture specific time and spectral domain properties of the sEMG signal and thus is a challenge for accurate classification of sEMG signals in human–device interfaces [106]. It has been shown that spectral variables, such as the mean (MDF) and median frequency (MNF), are reduced during sustained submaximal contractions whereas amplitude variables, such as root mean square (RMS), increase [106]. Methods suggested to minimize the effect of muscle fatigue include adaptive classifiers [107], on-line supervising mechanisms [90] and sEMG feature vectors (sEMG features are discussed in Section 3.2) that are robust against muscle fatigue [108].

3.1.4. The effect of segmentation strategies on the delay

Farrel [91,94] presented equations to estimate the worst, average and best case delays as well as delay ranges in the context of different segmentation strategies. These equations are presented in Table 1. The equations assume the transition between the contraction classes to be instantaneous but have still shown to produce accurate estimates of the controller delay [91]. The delay is a function of the window length, processing time, amount of window overlap, and the number of majority votes used. The window shift T_{new} is related to processing time τ, which is determined by the analysis window length T_a, processor, memory, type of features, algorithms used to extract features and perform pattern recognition, and the number of sEMG channels. Thus, the only parameters under the designer's direct control for a given feature set are the window length and the number of majority votes.

3.2. Features

Raw sEMG signals are mapped into smaller-dimension feature vectors because features describe the information content of the signal more efficiently than random and complex raw signal [21,43]. Because of the smaller size of the feature vectors, classifiers also perform faster, which improves the real-time properties of the system. EMG features can be grouped into four categories according to the domain where they are calculated:

1) time domain (TD) features,
2) frequency or spectral domain (FD) features,
3) time-scale or time-frequency domain (TFD) features and
4) spatial domain (SD) features.

Table 2 shows some features of each category. SD features can be calculated only from HD-sEMG conriqurations. A more detailed description of features, especially that of TD and FD features, can be found in Refs. [109,110].

Feature selection is the most important step in sEMG signal processing because the effect of the feature set on classification accuracy is even greater than the effect of the type of the classifier [7,125,126]. Three properties determine the quality of the feature space: maximum class separability, robustness, and computational complexity [110]. A high quality feature space results in clusters with maximum class separability or a minimum overlap, thus minimizing the misclassification rate. Robustness describes the ability of the feature space to preserve cluster separability in a noisy environment. The computational complexity of the feature set should be low so that the related procedure can be implemented with reasonable hardware and in real-time.

Although several studies have been made to find optimal features for classification of sEMG signals [93,109–111,118,121,122,127,128], few of these studies have made deeply quantitative comparisons of their qualities, particularly from the viewpoint of redundancy. In addition, there is little consensus between these studies because of significant differences in the study details: most notably, the number of postures classified, posture types and durations, data acquisition and the classification system used, the number of subjects and the data set sizes. Comparative studies have shown that TD features achieve higher accuracy for the LDA classifier, whereas TFD features outperformed them for the SVM classifier [104,129]. Considering the robustness of LDA over SVM, TD features classified with LDA have been suggested as optimal for sEMG classification [130]. However, this conclusion bases on studies made in low-noise laboratory conditions, and more study is needed to find the features capable to maintain high classification accuracy in real use. The classification system has also been shown to be subject dependent, and therefore it may be beneficial to tailor a classification system to each subject [78,79]. The following subsections describe the feasibility of each feature group in sEMG classification in more detail.

3.2.1. Time domain features

TD features are the most commonly used feature group in sEMG signal classification [36,42,81,93,113,114,125,131,132]. Their major advantage is that they are fast to calculate because no mathematical transformation is needed. However, because TD features are based on signal amplitude, they are relatively sensitive to noise and artifacts. Based on observations of scatter plots and mathematical properties, Phinyomark et al. [133] divided TD features into four main types: (1) energy and complexity information methods, (2) frequency information methods, (3) prediction model methods, and (4) time-dependence methods. Adding the features from the same category in the feature vector may increase the performance only slightly, due to small difference in feature space. Some features from each group are presented in Table 2.

There have been attempts to determine an optimal TD feature vector for several classifiers. Examples of TD feature vectors used in sEMG studies are presented in Table 3. The most common combination is the LDA classifier with Hudgin's feature vector consisting of mean absolute value (MAV), waveform length (WL), zero crossing (ZC), and signal slope changes (SSC) [42,93,95,100,122,134]. MAV estimates an average of absolute value of the EMG signal amplitude and WL, the cumulative length of the waveform over the time segment [74,110,133]. WL is a combined measure of signal amplitude, frequency and duration describing signal complexity. ZC is a number of times that amplitude values of the EMG signal cross zero amplitude level and SSC the number of times that slope of the EMG signal changes sign [74,109,110,135]. The benefits of Hudgin's feature set are relatively high classification accuracy, stability against changes in segment length, low discrepancy over several sessions, and computational simplicity [93]. In addition to LDA, it has also been shown to be an optimal TD feature vector at least for SVM and multilayer perception (MLP) [93].

It is also common to combine autoregressive (AR) coefficients with Hudgin's features (often referred to as the TDAR feature vector). This feature vector has shown high classification accuracy with LDA [7,8,60,64,89,136] MLP [137] and Gaussian mixture models (GMM) [125]. Autoregressive (AR) and Cepstral (CC) coefficients are two prediction model features used in sEMG signal classification for which AR coefficients are more commonly applied [109–111,115,118]. AR and CC coefficients are computationally more complex than other TD features and need longer segments, as described in Section 3.1.2. The larger the model order, the greater the computation time needed to determine the coefficients. Thus, the model should be kept as simple as possible without sacrificing classification accuracy. Previous studies have suggested 3rd [138], 4th [139] and 6th [132] AR order model as an optimal model for classification of movements from sEMG signals. The probability density function of sEMG amplitude has also shown promise as a TD feature permitting sEMG classification [140]. In a simulation study

Table 1
Equations to estimate worst-case, average, and best-case controller delay as well as difference between best- and worst-case controller delays.

Classifier type	Worst-case delay	Average delay	Best-case delay	Difference between best and worst case
No overlap, no majority voting	$D = \frac{1}{3}T_a + \tau$	$D = T_a + \tau$	$D = \frac{1}{2}T_a + \tau$	T_a
No overlap, with majority voting	$D = \left(\frac{n}{2} + 1\right) T_a + \tau$	$D = \left(\frac{n+1}{2}\right) T_a + \tau$	$D = \left(\frac{n}{2}\right) T_a + \tau$	T_a
Overlap, no majority voting	$D = \frac{1}{2}T_a + T_{new} + \tau$	$D = \frac{1}{2}T_a + \frac{n}{2}T_{new} + \tau$	$D = \frac{1}{2}T_a + \tau$	T_{new}
Overlap, with majority voting	$D = \frac{1}{2}T_a + \left(\frac{n+1}{2}\right) T_{new} + \tau$	$D = \frac{1}{2}T_a + \left(\frac{n}{2}\right) T_{new} + \tau$	$D = \frac{1}{2}T_a + \left(\frac{n+1}{2}\right) T_{new} + \tau$	T_{new}

Reproduced from Ref. [75], available: http://www.rehab.research.va.gov/jour/11/486/pdf/farrell486.pdf.
Note: General recommendation is that T_{new} is approximately an order of magnitude less than T_a, meaning that users should experience more consistent delay with overlapped windows. D = maximum delay between users intended movement and controller producing correct output class, n = number of majority votes, T_a = analysis window length, τ = processing time, T_{new} = amount of window overlap.

that classified sEMG data according to three force levels the core shape model outperformed higher order statistic combinations in all simulations due to the precise PDF shape screening embedded in its formalism.

3.2.2. Frequency domain features

Frequency domain (FD) features can be used to estimate muscle fatigue [141–144], force production [145] and changes in motor unit recruitment and firing patterns [43]. FD features are calculated from power spectral density (PSD), which can be estimated using Periodogram or parametric methods [146]. PDS is mainly determined by the firing rate of the recruited motor units in the low-frequency range (below 40 Hz), whereas the morphology of their MUAPs traveling along the respective muscle fibers mainly determines the high-frequency range (above 40 Hz) [147].

Phinyomark et al. [109] studied the properties of thirty-seven TD and FD features and found that TD features were superior to FD features. In addition to their poorer classification accuracy, FD features are computationally more complex than TD features. However, combining FD features with successful TD features may yield more robust classification than a feature vector consisting solely of TD features. Phinyomark et al. suggested mean frequency (MNF) as a potential candidate to combine with TD features because its discriminant pattern in the feature space is different from that of TD features [120]. Phinyomark et al. [121] modified the MNF and median frequency (MDF) features in order to increase the

Table 2
Some typical features used in sEMG classification. Notations: x_i = ith signal sample in a segment, N = number of samples in a segment, f_j = frequency of the spectrum at frequency bin j; P_j = the EMG power spectrum at frequency bin j; M = length of the frequency bin, A_j = amplitude.

	Mathematical definition	References
Time domain features		
Energy and complexity information methods		
Mean absolute value	$MAV = \frac{1}{N}\sum_{i=1}^{N}\lvert x_i\rvert$	[74,111]
Integrated EMG	$IEMG = \sum_{i=1}^{N}\lvert x_i\rvert$	[112,113]
Variance	$VAR = \frac{1}{N-1}\sum_{i=1}^{N} x_i^2$	[111,112]
Root mean square	$RMS = \sqrt{\frac{1}{N}\sum_{i=1}^{N} x_i^2}$	[8,110,114]
Waveform length	$WL = \sum_{i=1}^{N-1}\lvert x_{i+1} - x_i\rvert$	[74,113,115]
Log detector	$LOGDET = e^{1/N\sum_{i=1}^{N}\log(\lvert x_i\rvert)}$	[115]
Frequency information methods		
Zero crossing		[74,116]
Wilson amplitude	$WAMP = \sum_{t=1}^{N-1}[f(\lvert x_n - x_{n+1}\rvert)]$	[111,115,117]
	$SSC = \sum_{t=2}^{N-1}[f(\lvert(x_i - x_{i-1}) \times (x_i - x_{i+1})\rvert)]$	
Slope sign change	where $f(x) = \begin{cases} 1, & \text{if } x \geq \text{throshold} \\ 0, & \text{otherwise} \end{cases}$	[74,93]
Prediction model methods		
Autoregressive coefficients	$x_n = \sum_{i=1}^{P} a_{i,n}x_{n-i}$, P = model order, $a_{i,n}$ = ith AR coefficient at time instant n	[7,115]
Cepstral coefficients	$c_n = -a_n - \sum_{k=1}^{n}\left(1 - \frac{k}{n}\right)a_k c_{n-k}$, $c_1 = -a_1$, c_n = nth cepstrum coefficient, a_i = AR coefficient	[112,115]
Time-dependence methods		
Mean absolute value slope	$MAVS_i = MAV_{i+1} - MAV_i$; $i = 1, \ldots, K-1$; K = number of segments covering the signal	[109,118]
Histogram of EMG	HEMG divides elements in the EMG signal into equally spaced segments and returns number of signal elements for each segment.	[109,111,119]
Frequency domain features		
Mean frequency	$MNF = \sum_{j=1}^{M} f_j P_j / \sum_{j=1}^{M} P_j$	[120]
Median frequency	$\sum_{j=1}^{MDF} P_j = \sum_{j=MDF}^{M} P_j = \frac{1}{2}\sum_{j=1}^{M} P_j$	[120]
Modified mean frequency	$MMNF = \sum_{j=1}^{M} f_j A_j / \sum_{j=1}^{M} f_j A_j$	[121]
Time-frequency domain features		
Short time Fourier transform	$STFT(k, m) = \sum_{r=1}^{N-1} x(r)g(r-k)e^{-j2\pi mi/N}$; g = window function; k = time sample; m = frequency bins	[95,100]
Continuous wavelet transform	$WT_x(\tau, a) = \frac{1}{\sqrt{a}}\int x(t)\Psi\left(\frac{t-\tau}{a}\right)dt$; t = translation parameter; a = scale parameter; Ψ = mother wavelet function	[95,100,122]
Discrete wavelet transform	DWT splits the signal into an approximation and detail coefficients by passing it through complementary low- and high-pass filters. The approximation coefficients are further split into a second-level approximation and detail coefficients. By repeating the process, one signal is broken down into many lower resolution components.	[95,123,124]
Stationary wavelet transform	SWT does not decimate the signal at each stage, avoiding the problem of nonlinear distortion of the DWT and WPT.	[95]
Wavelet packet transform	WPT is a generalized version of DWT that is applied to both low-pass results (approximations) and high-pass results (details).	[95,98,100,122]
Spatial domain features		
Experimental periodogram	$\gamma(h) = \frac{1}{2n(h)}\sum_{i=1}^{n(h)}[x(z_i) - x(z_i + h)]^2$; h = distance vector, $x(z_i)$ = measurement at location z_i. $n(h)$ = number of pairs h units apart in the direction of the vector h	[76]

Table 3
TD feature vectors used in sEMG interfaces. H = healthy subject, A = amputee subject. 1 = classification accuracy under electrode location shift, 2 = classification accuracy under muscle contraction level change, 3 = classification accuracy with muscle fatigue. CKML =Cascaded-kernel learning machine, SE = sample entropy, AR6 = 6th order AR coefficients.

Feature vector	Classifier	Classification accuracy (%)	Classes	Bipolar electrodes	Subjects	Reference
MAV, WL, ZC, SSC	SVM	96	6	4	11H	[93]
MAV, WL, ZC, SSC, AR6	LDA	97	10	3	12H	[7]
MAV, WL, ZC, SSC, AR6, RMS	GMM	97	6	4	12H	[125]
MAV, WAMP, VAR, WL	ANN	98	12	32	1H	[117]
MAV, WAMP, AR, CC	LDA	70^1, 78^2, 87^3	4	2	8H	[115]
MAV, WL, AR, CC	LDA	70^1, 78^2, 88^3	4	2	8H	[115]
WL, LOGDET, AR, CC	LDA	70^1, 78^2, 88^3	4	2	8H	[115]
SE, CC, RMS, WL	LDA	98	11	4	4H	[130]
IEMG, WL, VAR, ZC, SSC, WAMP	GRA	96	11	7	12H	[113]
AR6, MAV	LDA	98H, 79A	11	4	5H, 5A	[132]
AR6, ZC	LDA	97H, 75A	11	4	5H, 5A	[132]
AR6, SSC	LDA	97H, 74A	11	4	5H, 5A	[132]
AR6, WL	LDA	98H, 79A	11	4	5H, 5A	[132]
AR6, RMS	SVM	96	6	4	11H	[93]
AR, HIST	CKLM	93A, 97H	8	3	2A, 1H	[119]

robustness property of these features by applying mean and median to the amplitude spectrum instead of the power spectrum because the variation of the amplitude spectrum is smaller. They compared the tolerance of sixteen traditional TD and FD features, and modified MNF and MDF features against white Gaussian noise. The results showed that a modified MNF is the most robust feature regarding white Gaussian noise. Therefore, modified MNF was suggested as a highly potential feature to augment the other features for a more powerful and robust feature vector. Recently, two novel FD features derived from discrete Fourier transform and muscle coordination has shown robustness against variations in contraction force [148].

3.2.3. Time-frequency domain features

Time-frequency domain (TFD) features used in sEMG classification include short time Fourier transform (STFT) [95,100,122], continuous Wavelet transform (CWT) [95,100,122], discrete wavelet transform (DWT) [95,123,124,133,149–152], wavelet packet transform (WPT) [95,98,100,122] and stationary wavelet transform (SWT) [95]. The drawback of STFT is that it cannot increase both time and frequency resolution simultaneously [153]. CWT, DWT and SWT overcome this deficiency by providing good frequency resolution with poor time resolution in low frequency band but poor frequency resolution with good time resolution in high frequency band [153]. Since DWT is computationally more efficient than CWT, it has become the most common TFD feature in sEMG interfaces. WPT has also gained interest because of its ability to provide the frequency information in both low frequency band and high frequency band. Although TFD features are computationally more complex than TD features, they can be implemented with fast algorithms that have shown to be capable to meet the real-time requirements in sEMG classification when appropriate dimensional reduction and segmentation techniques are used [92,98,122,152,154]. Wavelet transforms may improve the robustness of the system compared to TD and FD features because by using subsets of wavelet coefficients the analysis can be restricted only to interesting frequency bands.

TFD features yield a high-dimensional feature vector that requires dimensionality reduction transformation to increase the speed and accuracy of the classification. The most popular feature projection algorithms in sEMG signal classification are the principal component analysis (PCA) and uncorrelated LDA (ULDA) [100,103,129,155]. However, the feature extraction applied for wavelet coefficient is usually a TD technique [133,150,156,157]. TD features can be calculated either directly from the wavelet coefficients or the reconstructed sEMG signal [150]. Most studies of sEMG analysis have concluded the Daubechies wavelet family to be one of the most suitable for sEMG signal analysis [150,158,159]. Phinyomark et al. [120] compared several TD and FD features computed of the sEMG signal reconstructed using DWT coefficients of different levels. Useful feature vectors included a feature vector consisting of ZC, WAMP, and MAV computed of the second-level reconstructed sEMG signal with the Db7 wavelet and the Myopulse percentage rate (MYOP) feature of the first-level reconstructed sEMG signal with the Db8 wavelet [120]. Phinyomark et al. [156–158,160] have also suggested DWT as an optimal method to remove white Gaussian noise (WGN) from sEMG signals. Conventional filters cannot effectively remove WGN because its frequency components fall in the energy band of the physiological sEMG signal.

3.2.4. Spatial domain features

HD-sEMG measurements have made it possible to extract not only temporal and spectral but also spatial information from sEMG recordings. Spatial domain (SD) features would improve the differentiation between postures and force levels providing information about the spatial distribution of the MUAPs and on the load-sharing between muscles. The relevance of spatial information is supported by the observation that distinct regions of the muscle are activated differentially depending on the position of joint [161] as well as the duration [162] and strength [163] of the contraction. Since HD-sEMG has only recently adopted in the sEMG interfaces, very few studies have investigated and designed SD features for this purposes [75,76]. An example of SD feature is the experimental variodogram [76]. It has shown to yield classification accuracy comparable to the classical TD features but to be more robust against longitudinal and transverse electrode shifts [76]. Moreover, small variations in the number of measurements used to calculate the experimental variodogram do not change the number of points which form it, and consequently the feature space used in variodogram method [76]. Thus, the number of electrodes can be different during testing and training of the classifier which allows excluding the electrodes with poor signal quality from the computation of the variogram during the use of the sEMG interface without re-training the classifier.

3.3. Myoelectric control strategy

Two control strategies used in sEMG interfaces are pattern recognition-based and non-pattern recognition-based control. In pattern recognition-based control, a classifier is used to map the feature vector to a desired command, whereas non-pattern recognition-based control decides the control commands by comparing a value of a single feature to predetermined threshold(s).

Pattern classification-based approach is usually preferred in sEMG interfaces because it allows more versatile control scheme than non-pattern one. This subsection describes these sEMG control approaches.

3.3.1. Pattern recognition-based control

Pattern recognition-based approach relies on the assumption that the classifier is capable to recognize the input values introduced in the training session and assign each input value to one of a given set of classes. Input values are feature vectors calculated of the sEMG signal, and classes correspond to different control commands that are sent to the device. Pattern recognition has provided important improvements in sEMG control when compared to conventional non-pattern recognition-based control by extending the number DOFs and increasing the intuitiveness of control commands. sEMG pattern classification has been studied for decades [164,165], and several classifiers have been investigated and compared for use in sEMG control [93,114,126,134,166–170]. A detailed description of the most common classifiers used in sEMG interfaces is given in Refs. [43,118]. However, a number of comparative studies agree that with an appropriate feature set and a sufficient number of channels, most classifiers have similar classification accuracy [7,125,126,170]. The implication is that an appropriate feature representation makes the classification task a linear problem. The trend seems to be toward classifiers that are simple to implement, fast to train, and meet real-time contractions, such as LDA [8,50,58,64,91,92,130,171–174], support vector machines (SVM) [136,166,175], and hidden Markov models (HMM) [168,176,177], of which LDA is the most commonly used and has become a general recommendation for sEMG interfaces.

However, few studies have compared the ability of the classifiers to classify sEMG signals in long-term use and with additive artifacts or noise. It can be assumed that linear classifiers are more capable to maintain high classification accuracy compared to nonlinear ones because of their better capability to generalize sEMG data. Kaufmann et al. [178] demonstrated this by showing that The LDA classifier was the most robust against the long-term effect of fluctuating sEMG signals when compared to five state-of-art classifiers. sEMG data was recorded from 21 days, and the classification accuracy for LDA was 82.37% when trained with recent data and 78.73% when trained with data collected only during the first day. Young et al. [58] found that the LDA classifier also outperforms The MLP classifier when electrode shifts are present. However, more complex classifiers may be appropriate in long-term use where a proper classifier has to classify novel patterns during online training.

3.3.2. Non-pattern recognition-based control

Non-pattern-based controllers have simple structure, but the main limitation is that they allow only restricted number of control commands [43]. However, non-pattern recognition-based approach may provide an intuitive interface for navigation menus [26], wheelchairs [22] and assistive robots [179] that usually require fewer commands than, for example, multifunction control prostheses. The methods included in non-pattern recognition-based methods are proportional control [20,180], onset analysis [181–183], and finite state machines [22,184–186]. In proportional control, the strength of muscle contraction determines the speed or force of a device. Proportional control has been adopted in exoskeletons [20] and prostheses [180], where it is used with pattern recognition-based or other non-pattern recognition-based methods to control speed or force of an assistive device.

Onset analysis is performed either by using single-threshold or double-threshold methods. In the single-threshold method, the sEMG signal is compared with an amplitude threshold whose value depends on the mean power of the background noise [43]. This method is fast and simple to implement, but its high sensitivity to noise makes it suitable only for coarse ON/OFF detection. An adaptive threshold method, where the threshold is determined on the basis of the average power of previous sEMG contraction, has also been developed [179]. Thus, the threshold can automatically adjust itself when contraction power varies, so as to avoid misclassification. To perform a specific function, the user must produce a constant contraction to keep the sEMG amplitude above the associated threshold [43]. The single-threshold method can be based on a time-enveloped signal or instant signal value. In the first case, commonly used algorithms are signal mean value, low-pass-filtered signal mean value, or Marple–Horvat and Gilbey algorithm [187].

The single-threshold method is generally unsatisfactory because it strongly depends on the choice of the threshold [43]. To overcome this problem, the double-threshold method was developed [22,182]. It applies single-threshold detection to a fixed number of consecutive values of an auxiliary variable and detects onset when a certain number of auxiliary values cross the threshold. The double-threshold method (see Fig. 6) yields higher detection probability, which makes it superior to the single-threshold method [43]. However, the drawback of this method is that it is complex and computationally expensive. Therefore, Xu and Alder [183] developed an improved method based on the double-threshold method. The improved method is more sensitive, stabile and efficient with decreased computational cost. A detailed description of the method can be found in Ref. [183].

Finite state machine (FSM) based controller is described by a finite number of states, transitions between them, and commands. The states usually represent predefined commands for the device, and transition roles are associated with the signal features. In wheelchair [22,186] and assistive robot [188] control, FSM provides an intuitive, easy interface with high accuracy. An example of an FSM and the double-threshold-based signal-onset detection designed for the sEMG wheelchair is presented in Fig. 6. FSM has also been studied in upper limb prostheses [184,185], and the state-of-art commercial prostheses rely on FSM-based control. The effort required to control a prosthesis can be reduced by combining an FSM higher-level controller with pattern recognition-based approach [185]. In this control strategy, the patient must only initiate or stop a movement, and using information from local sensors, the low-level controller will control the movement.

4. Challenges and future trends

One of the major challenges related to the design of sEMG interfaces is to maintain high classification accuracy in long-term use. In real use, the muscle contractions, *i.e.* the classes associated to control commands, are performed in a variety of conditions, which may lead to differences in signal properties making them unrecognizable for the classifier. Another challenge is to develop a control strategy that allows simultaneous movement of multiple DOFs. This section describes the main challenges related to the design of sEMG interfaces and introduces potential approaches to overcome them.

4.1. Number of control commands

Although the pattern recognition-based method overcomes the non-pattern based one with the possibility to implement a more versatile user interface, increasing the number of control commands complicates the classification problem, which may reduce the classification accuracy. The number of classes investigated in sEMG studies usually remains fewer than twelve. When a maximum of 12 classes are examined, each additional output class included into the classification problem will cause the classification accuracy to drop by 0.26% [8].

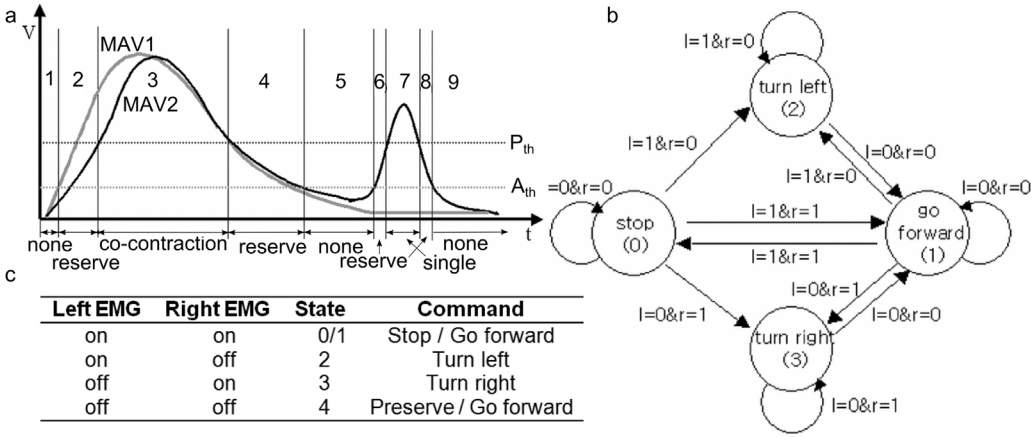

c

Left EMG	Right EMG	State	Command
on	on	0/1	Stop / Go forward
on	off	2	Turn left
off	on	3	Turn right
off	off	4	Preserve / Go forward

Fig. 6. EWP control using a finite state machine with the double-threshold method. (a) The double-threshold method is used to recognize shoulder elevation motions from MAV signals. P_{TH} and A_{TH} are the primary threshold and auxiliary threshold, respectively. If both signals are less than A_{TH}, as in (1), (5), and (9), that is recognized as no motion. If any signal is less than P_{TH} but above A_{TH}, as in (2), (4), (6), and (8) that is regarded as a transition state in which one or both muscles are relaxing from contraction or activating to contraction. In this case, the activation is reserved with the previous state. In the single-contraction state, only one signal exceeds P_{TH}, and another is less than A_{TH} as in (7). (b) State transition diagram for EPW control. (c) Definitions of motion states and commands by shoulder elevation motions. Left EMG and right EMG refer to the sEMG signal from the electrode placed on *the levator scapulae muscle* on the left and right sides of the shoulder, respectively.

For human–device interface purposes, increasing number of studies have combined sEMG information with information acquired from other sources, such as images [189], acceleration [190,191], voice [192], EOG signals [193], and EEG signals [194]. Utilizing multiple sensor modalities allows increasing the number of classes without compromising the classification accuracy significantly. Zhang et al. [195] managed to classify 72 Chinese Sign Language (CSL) words with average accuracies of 95.3% and 96.3% for two subjects by merging the information acquired by five sEMG sensors and a three-axis accelerometer. 40 CSL sentences were classified with an overall word accuracy of 93.1% and a sentence accuracy of 72.5%. The effective fusion of accelerometer and sEMG data was achieved using a decision tree and multistream HMM. The start and end points of sEMG signals of meaningful gesture segments were detected automatically on the basis of the intensity of the sEMG signals. These active segments were further segmented into analysis windows of 250 ms with 125 ms overlap and accelerometer signals were segmented synchronously with the sEMG signals. The feature vector consisting of 4th order AR coefficients and MAV was calculated from each analysis window of the sEMG signals. The sEMG signals were filtered between 20 Hz and 1 kHz, and sampled at 1 kHz. The accelerometer was placed on the back on the forearm near the wrist and five bipolar silver sEMG electrodes on the following forearm muscles: *extensor digiti minimi*, *palmaris longus*, *extensor carpi ulnaris*, *extensor carpi radialis*, and *brachioradialis*.

4.2. Simultaneous and proportional control

Pattern recognition-based classifiers can activate only one DOF at a time. This is a significant drawback, especially in prostheses where a user has to make a combination of sequential movements to perform a coordinated task. The strategies that have been used to apply pattern recognition-based classification to combined motions (*i.e.* activate multiple DOFs) are single, parallel and conditional parallel classification (see Fig. 7).

The single classification approach proposed by Davidge et al. [196] consists of one classifier in which each discrete (one DOF) and each combined motion (two DOFs) were labeled as separate classes. Braker et al. [197] introduced a parallel classification that predicts the classes with separate classifiers each of which is trained with discrete motions and a separate subset of channels. Young et al. [174] modified this method, using one classifier for each DOF and training the classifiers to discriminate between three classes, the two opposing motion classes of a DOF and no motion. Each motion class is trained using data from its discrete motion and, in contrast to the previous parallel approach, also using the combined motions in which it participates. The output is a combined action when two of the parallel classifiers have active motion classes as their output. This approach uses all channels for every classification decision. Young et al. [174] also developed a conditional parallel strategy that classifies each motion class with a separate classifier that discriminates between its designated discrete movement and all combined movements that have this discrete movement as a component. Thus, each classifier makes *a priori* assumption that one discrete motion class is active. The final output is the movement class selected by both of the conditional classifiers that contain the motion class. Each of the three classification strategies has been implemented using LDA classifiers and the parallel strategy also using SVM classifiers [198]. A comparison of LDA implementations shows that the conditional parallel classifier yields the best classification accuracy of the three approaches [174]. In classification of three DOFs, the conditional parallel strategy yielded error rates of 6.6% on discrete and 14.1% on combined motions, whereas for single classifier the corresponding values were 9.4% and 14.1%. Parallel strategy had the poorest performance, suggesting that it is not valid for all classification tasks. However, the problem of all these strategies is that they also need training data from combined motions. Limiting training to discrete motions is possible with the parallel approach, but it substantially increased the combined motion error to over 80% [174]. Training session becomes cumbersome, especially if the classifier needs retraining each time the device is used and the electrodes are replaced on the skin. Additionally, pattern recognition-based approach does not allow intrinsic proportional control.

Regression-based methods provide an alternative to pattern recognition-based control. Unlike classifier, regressor does not decide for a certain class but estimates a continuous output value for each DOF allowing an independent simultaneous and proportional control [199]. The idea of regression-based sEMG control is relatively new and most studies have focused on multilayer perceptrons for regression [137,200–202]. A regression of EMG *versus* kinematics requires training data for which the association between sEMG and kinematics is known. Obtaining this data from

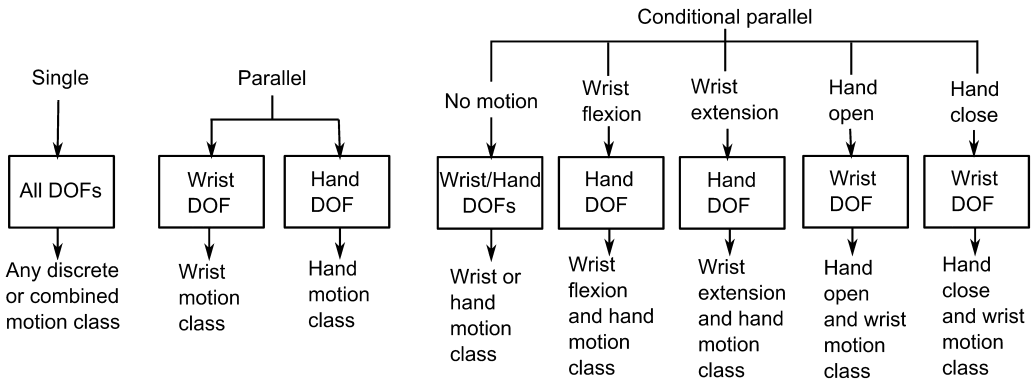

Fig. 7. Block diagrams of single (left), parallel (middle), and conditional parallel classification (right) strategies for two-DOF simultaneous wrist and hand movements. The number of DOFs can be increased by adding additional classifiers for the parallel and conditional parallel strategies. Each box represents a classifier with one or more DOFs. The single classifier discriminates all discrete and combined classes as separate motions. The parallel classification strategy classifies each DOF individually with two LDA classifiers. In the conditional parallel classifier strategy, each classifier has a class for specific discrete movement and classes for each combined movement in which the discrete movement is one of the two movements. The two classifiers that choose the same combination of motions determine the output of the conditional parallel classifiers. © [2011] IEEE. Adapted, with permission, from Ref. [174].

amputees is challenging since it is not possible to measure the kinematics of the missing limb. However, successful reproduction of hand kinematics has been achieved by learning the regression function from mirror movements where the kinematics are estimated from the able hand and the sEMG from the contralateral side with limb deficiency [137,200,201]. An alternative method is cueing the subjects on specific tasks and using the cues as labels [203]. Simple linear methods have shown to achieve performance comparable to those of state-of-art nonlinear regression methods at much lower computational demand for training and evaluation [204]. Especially Mixture of linear experts (EM), a physiologically inspired extension of linear regression, was suggested a promising candidate for sEMG control [204]. It can be easily realized on a simple inexpensive micro-controller with little power consumption and are readily modified for real-time adaptation. Moreover, EM yields high performance with relatively small amount training data.

Recently, the factorization of muscular activation patterns in weights and activation signals by non-negative matrix factorization (NMF) has gained special interest in the field of aEMG control research. According to muscle synergy theory, the extracted signals are related to supraspinal motor commands whereas the synergistic weights are determined by the spinal cord circuitries [205,206]. NMF-based method has demonstrated the feasibility of obtaining simultaneous and proportional control signals at multiple DOFs in healthy subjects [203,207], as well as amputees [208,209], both in offline analysis [207,208,210], and in online validations [208–210]. Since based on factorization, the procedure is in practice unsupervised, although a short initial calibration without labeled signals is required [208]. NMF-based approach also is appropriate for online adaptation since the synergy matrix can be re-estimated from any set of movements [208]. Moreover, it has been shown to be relatively robust with respect to the number and exact locations of electrodes and therefore targeting specific muscles is not needed [208].

A comparison of two supervised methods, ANN and linear regression, and a supervised method, NMF, revealed that despite the different capacity of mapping joint angles from the sEMG signals offline, the online performance of the three algorithms is similar [203]. This result indicates that an accurate mapping between sEMG and kinematics may not be necessary since an intuitive simultaneous and proportional control can be achieved by the continuous interaction and adaptation of the user with the sEMG controller through feedback. Similar observations have also been obtained in studies where the concept of "human embedded control" is used to describe the user's ability in controlling multi-DOF tasks through poorly calibrated controllers [211,212]. Thus, sEMG interface design should rather focus on a consistent mapping between sEMG and control strategies than an accurate estimate of physical variables.

4.3. Variation in limb posture

If sEMG signals are measured on the forearm, the variation in limb position associated with normal use can have a substantial impact on classification accuracy. Fougner et al. [191] showed that the classification error increased from 3.8% to 17.6% due to changes in posture and limb position. The degradation in the performance of the classifier during changes in limb posture can result from variety of reasons, such as electrode shift, variation of muscle recruitment due to gravitational forces, the force–length relationship of the muscle, and changes in musculotendon lever arm, which all depend on joint angles [213]. Even the muscle lengthening can change the efficiency of the muscle due to the degree of overlap of thin and thick filaments, causing an associated change in sEMG activity [214].

Chen et al. [172] proposed a solution to this problem by training a classifier in all possible limb positions. They succeeded in classifying seven hand and wrist postures in five upper limb positions, with an average classification accuracy of 88.8% using a LDA classifier and Hudgins feature set. The sEMG data was measured with six channels placed uniformly around the proximal portion of the forearm over the apex of the muscle bugle and the other two channels positioned on the distal end. The sEMG signals were segmented into windows of 300 ms with 100 ms overlap, band-pass filtered at the range of 20–450 Hz and sampled at the frequency of 4 kHz.

The same approach has also been extended by using accelerometers in addition to sEMG measurements [173,191]. Founger et al. [191] achieved a classification accuracy of 95% when the average value of the data measured by two analog 3-axis accelerometers was fed into the classifier as an extension of the sEMG features. Using only sEMG information, the classification accuracy was 94.3%. sEMG signals were acquired with eight pairs of electrodes embedded in a cuff placed around the dominant forearm, proximal to the elbow, at the position with largest muscle bulk. Accelerometers were placed over the *brachioradialis* muscle and over the *biceps brachii*. Both sEMG and accelerometer data were segmented using 250 ms windows with increments of 50 ms and sampled at 1 kHz. Additionally, the sEMG signals were low-pass filtered at 500 Hz. Although training a classifier with data from all limb positions

improves the performance compared to a classifier trained in one position, the drawback is a more complex and cumbersome training procedure. However, a promising result in the study of Founger at al. [191] was that for a test set of five positions, an increase from three to five training positions only yields a reduction from 5.3% to 4.9% in the associated classification error.

Boschmann and Platzner [50] studied the effect of the number of electrodes to distinguish 11 different hand and wrist postures recorded in three different upper limb positions. The measurements were made with an array of 96 monopolar electrodes (4×24) wrapped around the right forearm muscles, and the subset of electrodes used in measurements were selected symmetrically. When the classifier was trained all limb positions, classification accuracies of 90% were achieved with 4 sensors and 95% with 6 sensors. With 30 or more electrodes, the classification accuracy increased over 99%. The results were promising even with the classifier trained only in one upper limb position: the total average classification accuracy (*i.e.* includes both inter- and intra position classification accuracies) yielded over 90% with 20 or more electrodes. The sEMG signals were segmented using 100 ms windows with 50 ms overlaps, and Hudgins feature set was calculated from each segment. A LDA classifier was shown to slightly outperform SVM and *k*-nearest neighbor classifiers. However, the drawback is that increasing the number of electrodes also increases the production costs. In addition, the causes of degradation at different arm positions are different between healthy subjects (gravity compensation) and amputees (pressure change of the socket), and therefore more studies are needed to verify the capability of the approaches presented in this subsection for amputees.

4.4. Variation in contraction force

Variation in contraction force may introduce variation in the patterns of EMG signal measured during the same motion class [115]. Therefore, the classifier may not be able to recognize the motion class if it is performed at different force levels. Scheme et al. [177] demonstrated this with an experiment where 11 test subjects performed contractions at 20–80% of the strongest contraction they felt comfortable to produce. EMG data were collected with eight electrodes placed around the forearm during ten classes of hand and forearm postures and classified using A LDA classifier and Hudgins feature set. The presence of contractions from unseen force levels increased the error over 32% (a usable system should have an error rate under 10%). Introducing exemplars from all force levels in the training phase diminished the error substantially to 17% but required an extensive training session. One promising result was that a restricted protocol using only the lowest (20%) and highest (80%) force levels increased the error only marginally to 19% [177]. However, these results cannot be straightly generalized to amputee persons who have a different muscle structure after amputation and lack the visual feedback because of the loss of the limb. A study with two below-elbow amputees showed that it would be very difficult for amputees to control multiple forces for many postures without the proper adequate planned training to make them exert the correct pattern [215]. The classification error for amputees reduced from 60% to ~17% when the classifier was trained with all three force levels. The results were obtained with a LDA classifier and the feature vector consisting of integral absolute value (IAV), WL, ZC, SSC and kurtosis. The sEMG signals were acquired with 12 pairs of Ag/AgCl electrodes placed around the stump in 2 rows. The sampling rate was set at 2 kHz, and the sEMG signals were filtered using the band-pass filter of 20–450 Hz and notch filter of 50 Hz.

A recent study found that the orientation of muscle activation pattern vector of the frequency band is invariant for the same posture with different force levels [148]. Relying on this observation, two novel features robust to variations in contraction force were derived from discrete Fourier transform and muscle coordination [148]. These features achieved ~11% higher classification accuracy than two TD feature sets when classifying nine classes of postures with three different force levels using A LDA classifier. The sEMG data was acquired using 8 sEMG channels, the pand-pass filter of 20–450 Hz and the sampling rate of 2 kHz from the following muscles: *flexor pollicis longus*, *flexor digitorum superficialis*, *flexor digitorum profundus*, *abductor pollicis longus*, *extensor capri radialis*, *flexor capri ulnaris* and *extensor digitorum*.

4.5. Interface integrity with time

The factors that may alter the sEMG and thus challenge the robustness of the sEMG control system in long-term use include, external interference, electrode shifts with respect to the muscles, electrode impedance changes, sweat, the changes in muscle activity patterns and EMG signal properties due to fatigue and motor learning as well as variations in contraction force and limb position. Most of external interference, such as power line interference (especially problematic in monopolar recordings), can usually be removed with appropriate filtering. However, the sources of variation that are intrinsic to the system cannot be effectively suppressed. Online training has a high potential to allow the classifier to cope with these factors that may notably affect the sEMG patterns over time. In online training, a classifier can adapt to the variations in signal characteristics because it is trained continuously with new patterns during operation [43]. Updating the training data requires continuous evaluation of whether classified patterns coincide with user intentions. Entropy is suggested as an appropriate measure for this evaluation [216]. A potential approach for real-time classifier training is presented in [217]. The method is shown to allow stable discrimination of at least eight hand and forearm motions by adjusting to both gradual and drastic change in user's characteristics.

Classifiers based on neural networks have the potential to be used in online training [43]. For example, a very fast versatile elliptic basis function neural network (VEBFNN) would be powerful in training with incoming patterns during online training because it can learn data sets accurately in only one epoch and discard them after passing through [218,219]. This training procedure is fast in comparison to the traditional neural networks and needs only a small amount of memory [219]. VEBFNN has shown to be effective in facial sEMG feature classification [218]. Another classifier appropriate for online training would be fuzzy adaptive resonance theory mapping (fuzzy ARTMAP) that is fast, plastic and stabile, as well as able to generally achieve better accuracy over a smaller number of processing nodes [43,220]. A modified version of fuzzy ARTMAP, used to classify sEMG signals, is discussed in [220].

5. Applications

In recent years, the interest toward sEMG interfaces has rapidly increased, as can be seen from Fig. 8. The main reason for this is that pattern recognition-based control strategy was adopted in sEMG interfaces in 1993 [74]. The most important application areas of sEMG interfaces are assistive technology, rehabilitation technology, mobile technology, and silent speech recognition. This section reviews the state-of-art applications of each category.

5.1. Assistive technology

In the field of assistive technology, EMG interfaces have been adopted in prostheses, wheelchairs and assistive robots. This section describes the results achieved by EMG control in these applications.

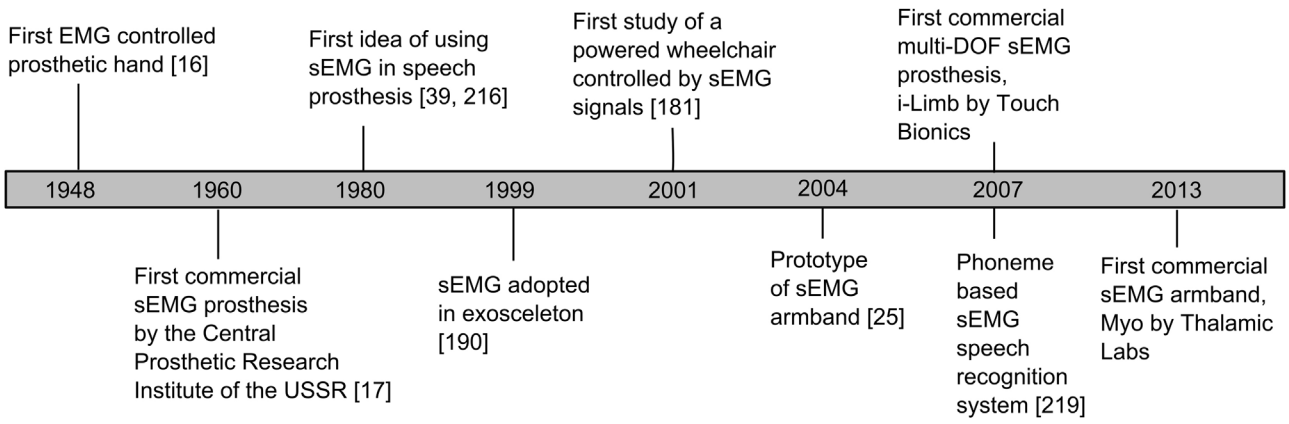

Fig. 8. Timeline for sEMG applications.

5.1.1. Prostheses

sEMG prostheses are the most-studied application of sEMG interfaces [94,103,110,125,134,166,167,176,184,198,221,222]. The use of sEMG in upper limb prostheses dates back to the 1960s when the first commercial prosthetic arm was developed by the Central Prosthetic Research Institute of the USSR [17]. It had one DOF, opening and closing, that was controlled with strong contraction of antagonistic muscles. Despite sEMG studies having reported high classification accuracies (>98%) achieved up to twelve classes [36,117], the threshold based principles of the early systems are still applied by clinically and commercially available sEMG upper limb prostheses in the present day. The simplest control approach is threshold-based on/off-control where the desired function is actuated when the sEMG amplitude exceeds the predefined threshold value. In this approach, different functions can also be assigned to different channels placed on the physiologically appropriate muscles. However, at least two signal sites are required to control one DOF (*e.g.* hand open/close). Alternatively, the range of muscle activity, from the detection threshold to the value at maximal contraction, can be divided into several intervals, each corresponding to a prosthetic function [223]. Other strategies applied in commercial prostheses are rate coding where the speed of the muscle contraction is associated with the desired functions (*i.e.* slow contraction selects one function a fast another) and pulse coding where the control command are pulses of sEMG activity (*i.e.* one pulse corresponds hand open, two pulses hand close) [223].

The commercial prostheses remained relatively unchanged until 2007 when, the first upper limb prosthesis with five individually powered digits, was launched (i-Limb, Touch Bionics, Livingston, U.K., http://www.touchbionics.com/). Since that also other prostheses with multiple DOFs have entered the market for patients (Fig. 9.). These systems usually exploit finite-state-machines and employ only two sEMG signals intended to use for both DOFs and the switches from one DOF to another. Thus, DOFs are controlled in a serial fashion and require unintuitive movements to produce both the control signals and the co-contractions needed to toggle between the different DOFs. Moreover, the approach does not allow simultaneous control of multiple joints and becomes cumbersome if the DOFs are increased.

The main barrier that prevents adoption of the pattern recognition-based approach for clinical use is the concern over long-term system robustness. For example, effects of socket loading and limb orientation [173], variations in muscle contraction effort [115], and electrode shifts [59] during donning and doffing as well as during use result in changes in the EMG and will cause the classifier to be operated with signals different from those used to train it. Moreover, most studies have used healthy subjects, and more study is needed to ensure robust classification also with amputees. Another significant challenge in the design of multifunctional prostheses is their power-weight ratio: The state-of-art non-prosthetic mechanical hands have 20 degrees of freedom (human hand has 24 degrees of freedom), but they cannot be used as prostheses because their actuation and control system are too heavy and bulky [224].

5.1.2. Electric power wheelchairs

The first publication on sEMG-controlled electric power wheelchair EPW is from the year 2001 [225], and thereafter several prototypes have been designed [22,186,192,226–228]. Generally, a myoelectric wheelchair interface includes the following control commands: go forward, go backward, turn left, turn right, and stop [22,186,192,227]. Only TD and FD features have been used in EWPs because of their better real-time properties compared to TFD features. However, discrete wavelet transform can be computed relatively quickly with currently available hardware, and thus it may also be appropriate for EPWs. Because the control of EPWs requires relatively few commands, even simple non-pattern recognition-based control strategies have provided easy and effective sEMG interface for EPWs [22,186,192]. Although computational simplicity has made non-pattern recognition-based methods popular in EPWs, the development of microcontrollers and microprocessors has increased the interest toward pattern recognition-based control strategies [226–228]. For example, Song et al. applied a fuzzy Min–Max Neural Network (FMMNN) to drive an EPW based on the sEMG signals collected from the forearm muscles [226]. The control system adjusted the min–max values of the hyperboxes in FMMNN according to the sEMG feature variation for every 2 s making the system robust against muscle fatigue. The variation in the sEMG features caused by muscle fatigue was evaluated with MDF and MNF. The sEMG feature vector used as an input to the classifier consisted of difference absolute mean value (*i.e.* the mean absolute value of difference between adjacent samples), IAV, ZC and VAR. The features were calculated from the segments of 128 ms. The sEMG signals were filtered within the range of 20–500 Hz and power-line noise was reduced with 60 Hz notch filter. The sampling rate was set to 1 kHz.

A suitable place for electrodes for EPW control purposes is, for example, on shoulder muscles, because the shoulder elevation motion is distinct from gestures used in daily living [22,192]. The other common places for electrodes are the muscles in forehead [189], face [229], neck [22,227,230], forearm [228,230], and hand [231], depending on the ability of the patient. Also a system that allows a reliable control over one arbitrary muscle group has been developed [186]. The number of channels used in sEMG-controlled EPWs varies between 1 and 4 [227,228,232]. Generally, the classification accuracies yielded in the studies of sEMG-controlled EPWs are over 90% [22,227,229,232]. In EPWs, it is also common to

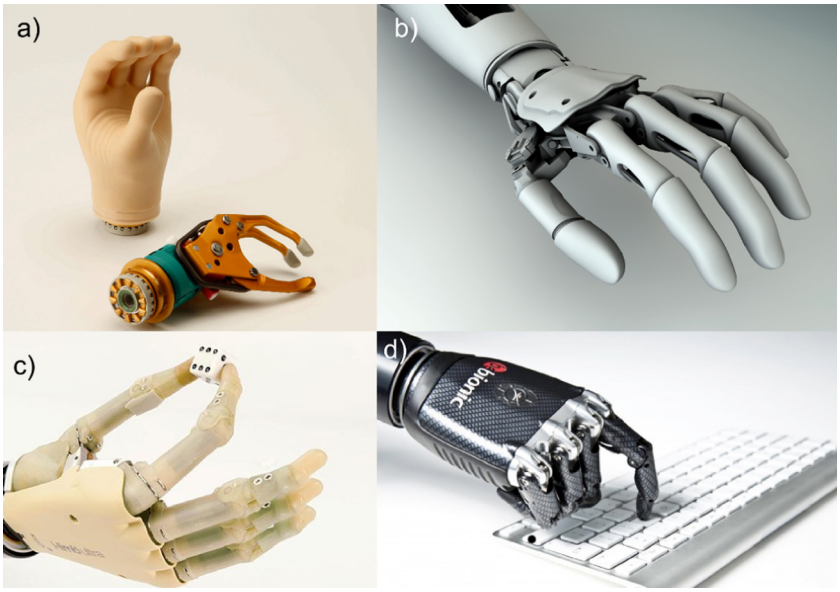

Fig. 9. Examples of commercial prosthetic hands: (a) Sensor Hand Speed (© Otto Bock, Duderstadt, Germany). Reprinted with permission. (b) Michelangelo (© Otto Bock, Duderstadt, Germany. Reprinted with permission). (c) I-Limb Ultra (© Touch Bionics, Livingston, U.K. Reprinted with permission) and (d) Bebionic (© RLS Steeper, U.K., Leeds. Reprinted with permission).

combine the sEMG information to the information achieved from color images of face [189], voice commands [192], EOG signals [193], or EEG signals [194].

5.1.3. Assistive robots

Assistive robots are a less-studied application of sEMG interface in the field of assistive technology [179,216,233]. An example of an assistive robot is sEMG controlled meal-assistance robot developed by Zhang et al. [179]. The robotic system is designed for people with disabled upper limbs. When the subject contracts his/her muscle, the robot will pick up the food in the selected tray and feed the subject. sEMG signals were measured with four bipolar electrodes placed on the calfs and shoulders, amplified, sampled at the sampling rate of 500 Hz, and high-pass filtered with a cut-off at 120 Hz. The onset of the muscular contraction is detected by an online algorithm with adaptive sEMG power threshold and the output of onset analysis is converted into appropriate command. Compared with joystick controls, the sEMG control system had a good performance in preciseness, efficiency and comfort when tested with healthy subjects. When excluding one subject, who had an especially low rate of success, the mean rate of success of sEMG control outperforms the joystick control with 95.2% *versus* 93.7%.

5.2. Rehabilitative technology

Applications of sEMG interfaces in the field of rehabilitative technology include sEMG-driven exoskeletons [234–238] and serious or applied games [24,239,240]. This section overviews the use of EMG control in these applications.

5.2.1. Exoskeletons

The first publication about an sEMG-driven exoskeleton dates back to 1999 [234], and since then several prototypes of sEMG-based exoskeletons have been developed for rehabilitation and assisting of physically weak persons including the elderly and individuals who sustain neurological impairments, such as spinal cord injuries, acquired brain injuries, or stroke. In exoskeletons, the sEMG measurements can be used as an indicator of the effort generation to trigger assistance [241] or to compensate the weakness of the muscles by generating assisting forces proportional to the amplitude of the sEMG signal [20,242]. One of the two typical control approaches considered for exoskeleton control is the neuro-fuzzy method [243–248]. Its drawback, however, is that the control rules become complicated if the degree of freedom of power-assist is increased. The other typical control method relies on the estimate of joint torque needed to perform the movement [234–237]. However, torque-estimating methods usually relate to complex subject- and session-dependent calibrations which confine their use to laboratory conditions.

Lenzi et al. [242] showed that an accurate estimate of muscle torque is unnecessary for providing effective movement assistance since the user is able to adapt to the imprecision of the control system. They developed a proportional sEMG-based control system for an elbow-powered exoskeleton that gives only a rough estimate of the user's muscular torque and does not need any specific calibration. The system obtained linear envelope from the raw sEMG signals online through full-wave rectification of the band-passed sEMG signals and postfiltering by means of a second-order low-pass Butterworth filter with a cut-off frequency of 3 Hz. Thereafter, the force set-points for the flexor and extensor actuators of the exoskeleton were obtained by multiplying the linear envelopes with two different constant factors. The closed-loop low-level controller regulated the cable forces for flexor and extensor actuators to produce the final assistive torque on the user joint. The assistive torque artificially strengths the muscle proportionally to the intensity of the muscle activation. The sEMG signals were acquired by bipolar Ag/AgCl electrodes placed on the *biceps brachii* and *triceps brachii* muscles. Experimental results show that subjects adapted almost instantaneously to the assistance provided by the robot and could reduce their effort while keeping full control under different dynamic conditions.

5.2.2. Serious games

A serious game is a game the primary purpose of which is other than pure entertainment. sEMG controlled serious games can be used to motivate patients in physical exercises and provide a distraction from pain or anxiety [24,239,240]. An example of sEMG controlled serious game is a biofeedback system for muscle rehabilitation [240] developed by Lyons et al. Based on the intensity of muscle activity recorded from the muscle of interest, the

system enables or disables the playing of a computer game by a user. The hardware consisted of a bipolar detection EMG amplifier unit and a Desktop unit. The amplifier provided a band-pass filtered (20–500 Hz) raw sEMG signal to the Desktop unit that generates a linear envelope representation of the sEMG signal. The system software read the linear envelope of the sEMG signal from the desktop unit and using a custom threshold level, determine whether game play was enabled or not for the user.

5.3. Input devices

Human–device communication technologies currently use mainly physical transducers such as mice, keyboards, pens and joysticks in their mediation. However, as technology is being integrated more seamlessly into our environment, situations arise where direct manipulation of a physical input device may be inconvenient or difficult. This section discusses the benefits of sEMG control over traditional input devices and reviews the results achieved with applications which have adopted the sEMG interface.

5.3.1. Armbands for mobile devices

sEMG armbands have been developed to replace the traditional input devices in situations where hands are busy or where private interaction without disruption to the immediate environment is desired (see Fig. 10) [25–27,29,30]. Constanza et al. [26] developed a myoelectric motionless gesture sensor that detected isometric muscular activity (*i.e.* muscular activity that does not produce movement) allowing discreet and unobtrusive interaction with mobile devices. The device was inserted into an elastic armband made for a commercial MP3 digital music player, as shown in Fig. 10. The system also provided tactile feedback about the gesture being recognized. The subtle gestures were modeled as short bursts of activity preceded and followed by inactivity in the standard derivation of the sEMG signal [26,27]. The standard derivation was computed over a sliding window of 0.2 s with 75% overlap. When the activation was detected, the controller sent a signal wirelessly to the main wearable processing unit, such as mobile phone. sEMG signals were measured by wet bipolar Ag/AgCl electrodes placed around the upper arm [26]. The prototype was validated in an experiment where subjects selected items from an audio menu through subtle gestures while a simulated mobile task. The results showed the sEMG interface can be used to discretely interact with a device without being detected by others. The classification accuracies were 97.6% for condition where two armbands were used in two arms and 94.6% for the condition whit single armband.

Saponas et al. [29] from Microsoft have also studied the feasibility of sEMG interfaces in mobile applications by developing a prototype of an armband capable of sensing a variety of finger gestures. The prototype worn on the upper forearm (see Fig. 10c) consists of an embedded wireless muscle-sensing device combined with electrodes and a sports sweatband. The circular electrodes were arranged into two sets of three bipolar electrode pairs; one set on top of the forearm, the other set on the bottom. The sEMG signals were classified at segments of 32 samples using an SVM classifier. From each segment a feature vector consisting of the amplitude of each channel as the RMS amplitude of the fully rectified signal, the RMS ratios among all six channels, spectral power in several frequency bands, the ratio of high-frequency energy to low-frequency energy within each channel, and the phase coherence among each pair of channels. The prototype was tested in an experiment where eight subjects were asked to pinch with one of three fingers. Their system performed best at recognizing the pinching gesture, with the mean accuracy of 86% when collecting training data immediately after testing, 87% when the data was collected after a short break and 86% when using training data from the previous day. The classification accuracy of pressing gestures was much poorer, with mean accuracies for the same session, short break and one-day break of 76%, 73%, and 66%, respectively.

5.3.2. Muscle computer interfaces

sEMG interfaces have advantages over traditional input devices in computers, and sEMG counterparts have been developed for example to mouse controllers, joysticks and keypads [28,249]. Current input devices are usually relatively complex to use because numerous physical buttons and sticks need to be manipulated simultaneously. sEMG interface may decrease the complexity since it allows mapping of multiple muscle groups to different actions.

The researchers at the Neuroengineering lab at NASA demonstrated the feasibility of sEMG sleeve to replace traditional joystick and keypad in space-based applications (see Fig. 11) [28,250]. In the first experiment, the sEMG signals were associated to joystick commands for a realistic flight simulator for an airplane [250]. The sEMG signals were acquired by four dry differential electrode pairs mounted in a sleeve on the subject's forearm. In the second experiment, the subject pretended to type on a numerical keypad, and the sEMG signals were processed to keystrokes [250]. However, to improve the signal-to-noise ratio, eight pairs of wet electrodes were used instead of the sleeve with dry electrodes. One ring of wet electrodes was placed near the wrist and another near the elbow. In both experiments, the sEMG signals were amplified with the gain of 2000, filtered with antialiasing filter, and sampled at 2 kHz with 16-bit precision. Moving averages of the segmented sEMG signals were computed, and the resulting feature vectors were classified with four HMMs in the joystick experiment and with 11 HMMs in the keypad experiment. Each HMM was trained for a particular gesture. The results demonstrated the feasibility of sEMG control while indicating the need for further research to reduce the incidence of errors. Future visions of the pattern recognition software were planned to be capable of adapting to the preferences and day-to-day variations in sEMG signals of individual users.

Researchers at Microsoft have studied sEMG control to increase the interaction vocabulary available for existing human–machine communication. A prototype of a muscle-sensing interactive surface by Microsoft is able to provide information about which fingers are touching the surface, the amount of pressure exerted, and gestures that occur when not in contact with the surface [251]. The sEMG signals were recorded at 2048 Hz using six circular gel electrodes and two ground electrodes placed in a roughly uniform ring around the upper forearm of the user's dominant hand. Additionally, coarse muscle activation was measured by two electrodes placed on the forearm of the non-dominant hand. The data was divided in 250 ms segments each of which filtered between 2 and 102 Hz. The 60 Hz noise was reduced with notch filter. The feature vector and classifier were same as in Microsoft's sEMG armband described in Section 5.3.1. The utility of sEMG sensing surface was evaluated in an experiment where test subjects performed drawing and editing tasks (*i.e.* copy, pick, move/cut, undo) with four sEMG-based interaction techniques: pressure sensitive painting (more pressure results in darker strokes), finger-aware painting (different colors were associated with the index and middle fingers), finger-dependent pick and throw (the pinch and throw gesture primitives to cut/copy and paste operations) and undo flick (flick gesture performed by the non-dominant hand was associated to the undo operation). Five of six subjects performed all drawing and editing tasks without problems. However, the system requires gross calibration each time a user dons the device.

The increased interaction vocabulary also allows designing games more realistically. Muscleman, a wireless input device for a fighting action game, acquires the sEMG of the flexor muscle in the forearm with dry Ag/AgCl electrode and uses the force of the contraction as an input [252, web publication, avaliable: http://www.intuinno.com/uploads/1/0/2/9/10297987/muscleman_paper.pdf,

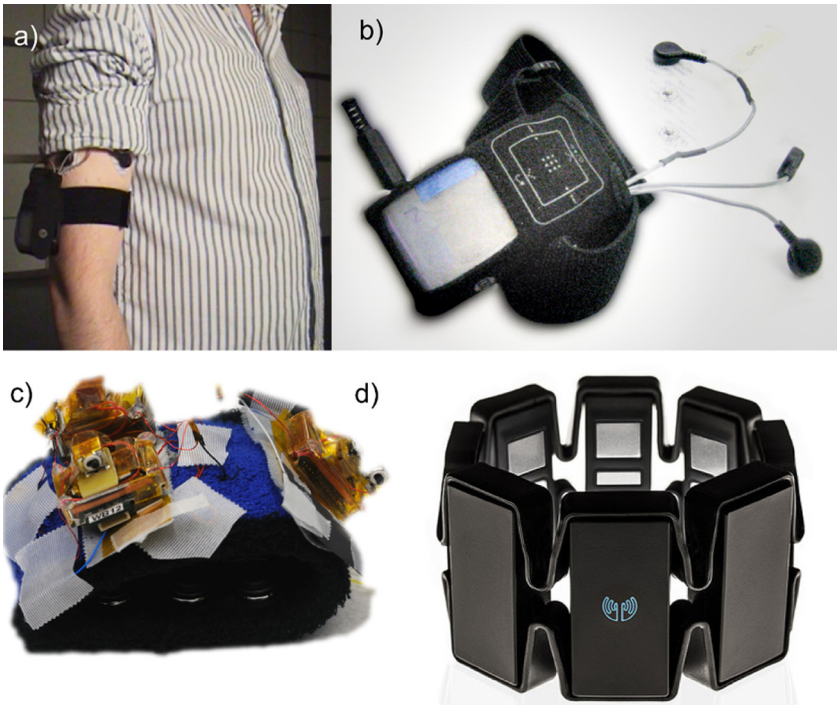

Fig. 10. sEMG-controlled armbands: (a) and (b) the prototype of the sEMG sensor inside an armband holder for commercial digital music player [26] (reproduced with permission from PhD. Enrico Costanza, the Agents, Interaction and Complexity (AIC) Group in Electronics and Computer Science at the University of Southampton (UK)), (c) the prototype of the myoelectric armband developed by Microsoft [29] (reproduced with permission from Ph.D. T. Scott Sapoans, Microsoft Research, Redmond, United States of America) and (d) the first commercial sEMG armband, Myo (© Thalamic Labs Inc., Ontario, Canada. Reprinted with permission.). Myo combines the information collected by sEMG electrodes and the 9-axis inertial measurement unit (IMU).

http://www.intuinno.com/muscleman.html]. sEMG signals were sampled at 450 Hz and band-limited to 30–300 Hz. RMS was calculated from the sEMG signal to evaluate the muscle contraction force. In the calibration, the sEMG was measured from the forearm of the user during relaxation and during the maximum isometric contraction. These two values were used to normalize the RMS values when the game is played. By using muscle contraction as an indication of force, the user can intuitively make light or heavy level version of the two attaches. The attaches were classified using accelerometer data.

5.4. Silent speech recognition

Silent speech interface (SSI) has shown promise to overcome conventional speech recognition in acoustically harsh environments or in situations where private communication is desired [28,38,39,168,253–256]. SSI captures silent speech by analyzing sEMG signals measured on the skin surface around the region of articulatory muscles in the face and neck. Thus, measurable signals still occur when a subject emits a few or no acoustical signals avoiding the disturbance of bystanders and ensuring robust speech

Fig. 11. An sEMG-controlled keypad (left) and a joystick (right) developed by NASA.
© [2010] IEEE. Adapted, with permission, from Ref. [28].

signal transmission in adverse environmental conditions. SSI may also help persons who have undergone a laryngectomy (vocal cord removal) or elderly people for whom speaking requires a substantial effort.

The first publications about the sEMG-based speech recognition appeared already in the mid 1980s [39,254]. However, for vocabularies over 10 words, the recognition accuracy remained below 70% [254,257] until 2001 when Chan et al. [253] achieved classification accuracies of 97% and 90% for two subjects on a 10-word vocabulary of English digits. They used five pairs of gel Ag/AgCl electrodes to measure sEMG signals from five facial muscles: *levator anguli oris*, *zygomaticus major platysma*, *depressor anguli oris and anterior belly of the digastric*. The signals were first fed into pre-amplifier with the gain of 600 and into amplifiers with a frequency range at 10–1000 Hz and gain varied between 10 and 50. Thereafter, the sEMG signals were low-pass filtered at 500 Hz and sampled at 1 kHz using a 12 bit ADC board. Hudgins' TD features derived from Wavelet Transform were computed from the segments of 1024 samples, and after dimension reduction with PCA the feature vectors were classified with A LDA classifier.

However, these studies investigated only audible speech, and it remains unclear if the results can be generalized to the silent speech. Little is known about the articulation differences between silent and audible speech, but there is evidence that sEMG signals measured during silent and audible speech are significantly different from each other [258]. Despite the possible differences, Jorgensen et al. [255] showed promising results even when no acoustic signal was produced. In 2003, they succeed in classifying six sub-acoustic words with up to 92% accuracy. sEMG signals were collected using two pairs of wet self-adhesive Ag/AgCl electrodes placed on the left and right anterior area of the throat ~250 mm back from the chin cleft and 1–0.5 cm from the right and left side of the larynx. sEMG signals were sampled at 2000 Hz and notch-filtered to remove ambient interference of 60 Hz. Several sEMG features were compared of which Kingsbury's Dual Tree Complex Wavelet yielded the highest classification accuracy. The feature vectors were classified with Neural Network classifier.

Recognizing continuous speech and a larger vocabulary requires breaking words into sub-word units, such as syllables, phonemes, or context-dependent model units. Scheme et al. demonstrate a phoneme-based word recognition system in 2007 [259]. They used an HMM classifier, in which each model represented a new phoneme. This allows adding a new word without building and training a new HMM if the phonemes in the new word are already represented by existing HMMs. HMM was trained with single Gaussian mixture observation densities using Forward–Backward algorithm for each phoneme. Because sEMG was unique to each subject, speaker dependent models were needed. sEMG signals were recorded with five bipolar Ag/AgCl electrodes attached over five articulatory muscles: *levator anguli oris*, *zygomaticus*, *platysma*, *depressor anguli oris*, and *anterior belly of digastricus*. 16 bit AD converter digitized the signals sampled at 5 kHz. An 18-phoneme vocabulary, which contained words from "zero" to "nine" was classified with an accuracy of 95%.

The large number of classes challenges the reliable classification in SSIs. In general, the classification approaches and feature vectors used in SSI studies have been more complex compared to ones used in other sEMG applications. There also is evidence that simple TD features that have provided high performance in classifying gross movements may not be optimal for SSIs [260]. The idea of sEMG-based speech recognition is still in research, and more study is needed to find features that that can be classified accurately in real-time.

6. Conclusion

sEMG interface picks up electrical activity on the skin surface with electrodes during a voluntary muscle contraction and decodes the sEMG signals to the commands sent to the device. This review presented a summary of the recommended methods for the critical steps of digital sEMG signal processing. Additionally, it discussed the major challenges and future trends of sEMG interfaces as well as the state-of-art applications where sEMG interfaces have been adopted.

Important issues to consider when designing an sEMG interface are related to acquiring sEMG signals with electrodes, as well as filtering, segmentation, feature extraction and classification of the sEMG signal. Because the general recommendations for electrode configurations, presented for example by SEMIAM, are designed for measurements in laboratory conditions, they may not always be optimal for sEMG interfaces where the purpose is robust signal classification during long-term use in real use environments. Relatively global sEMG measurements from a muscle group have been found to include sufficient discriminatory information for successful classification. Thus, it is not always necessary to target the electrodes to specific sites on single muscle(s); it can be enough to place electrodes on the muscle group of interest. The optimal number of sEMG channels for hand and forearm posture recognition can vary, but it is suggested to be between four and six bipolar channels. The recommended electrode size is about 1 cm × 1 cm or 2 cm × 2 cm. If electrode shifts are present, higher classification accuracy may be achieved by increasing the inter-electrode distance from the generally used distance of 2–4 cm. HD-sEMG with arrays of multiple electrodes provides a promising alternative to conventional bipolar measurements since it allows designing sEMG interface that is relatively tolerant against electrode displacements and does not require re-training if malfunctioning electrodes are removed during the use of the sEMG interface. In HD-sEMG systems the IED should be below 10 mm to avoid spatial aliasing. However, the optimal sEMG setup is muscle-, muscle-group-, and task-specific, and thus need to be customized for the purpose used.

Because most of the energy of sEMG signal is below 400–500 Hz, sEMG studies have usually adopted the sampling rate of 1000 Hz and the high-pass cutoff frequency of 20 Hz. However, recent evidence suggests that an accurate classification is possible with a more narrow frequency range, with sampling at 500 Hz and high-pass cutoff at 60 Hz. With these values, the processing time and the need for memory can be halved. The classification accuracy of the sEMG system may be further improved by using preprocessing algorithms, such as ICA and cPCA.

Delay should be minimized in real-time sEMG applications. Equations have been presented to estimate the worst, average and best case delays as well as delay ranges. A delay is a function of the window length, processing time, amount of window overlap, and the number of majority votes used. Shortening the length of the segments decreases classification accuracy. The theoretical minimum for a segment length is 200 ms, but shorter segments can be used with MV. No obvious difference exists in classification accuracy whether it is used a large window with a small number of votes or a small window with a large number of votes, but less storage space is needed in the latter case. Overlapped segmentation is the optimal segmentation strategy. Although classification relying on steady-state information has been shown to be superior compared to classification based on transient data, dynamic portions of EMG signals also are important for real myocontrol systems and thus must be included in the learning process in order to achieve high overall classification accuracy.

sEMG commands can be decoded using pattern recognition-based methods or non-pattern recognition-based methods, and also both of them can be adopted in the same system. Non-pattern

based methods are more simple to implement and may be effective in navigation menus, wheelchairs, and assistive robots. If the purpose is to control multiple DOFs, pattern recognition-based methods are more appropriate. However, today most studies concentrate on the pattern recognition-based control approach because it allows a more versatile user interface. The recommended classifier in sEMG interfaces is LDA, because it does not require any parameter adjustment, is computationally efficient and robust and yields similar classification accuracy to that of more complex classification algorithms.

The most critical step in sEMG signal processing is feature selection. The optimal feature set depends on the measurement system as a whole as well as on the classification task. The A LDA classifier with the TDAR feature set (*i.e.* MAV, WL, SSC, ZC and AR coefficients) has become a common combination in sEMG studies. The drawback of TD features, however, is that they are based on signal amplitude, which makes them relatively sensitive to noise. FD features have poorer classification accuracy than TD features but are suggested as augmenting features for successful TD features to increase the robustness of the feature set. Extracting TD and FD features from DWT coefficients or from the signal reconstructed after wavelet denoising may also increase the robustness. HD-sEMG, recently adopted in sEMG interfaces, allows the study of the sEMG signal in the spatial domain, opening new possibilities to the field of sEMG control.

sEMG interfaces have numerous applications, which can be divided into four application areas: assistive technology, rehabilitation technology, input devices, and silent speech recognition. Most research on sEMG interfaces has concentrated on the applications of assistive and rehabilitation technology, but in the recent years the interest has also increased in sEMG applications for healthy people. Examples of the applications where sEMG interfaces have been used include prostheses, exoskeletons, silent speech interfaces, and armbands that replace traditional input devices.

sEMG interface provides a totally new way of communication that will open up possibilities to comprehensive human–device interaction. The advantages that it offers to the user over existing control methods include subtle and intimate communication, independence of portable control devices, and avoidance of direct eye contact or deep attention by the user. The major challenge in developing the prototypes of sEMG applications to commercial products is to achieve robust classification in long-term use without making the classifier training procedure too cumbersome. While relatively simple classifiers and feature vectors have been sufficient to provide high classification accuracy in laboratory conditions, the future trend in sEMG studies seems to be toward more complicated control systems, such as conditional parallel classifiers, regression-based methods, signal factorization as well as utilization of online training and sensor fusion (*i.e.* using sEMG with other sensor modalities) that are likely to allow more robust and versatile user interface.

Acknowledgements

This study has been supported by the Foundation for Aalto University Science and Technology (Celebratory gifts' fund to Maria Hakonen), the Academy of Finland (grant #13266133 to Harri Piitulainen), and by the SalWe Research Program for Mind and Body (Tekes – the Finnish Funding Agency for Technology and Innovation grant 1104/10).

References

[1] L. Fehr, W.E. Langbein, S.B. Skaar, Adequacy of power wheelchair control interfaces for persons with severe disabilities: a clinical survey, J. Rehabil. Res. Dev. 37 (3) (2000) 353–360, ISSN: 07487711.

[2] M. Al-Rousan, K. Assaleh, A wavelet- and neural network-based voice system for a smart wheelchair control, J. Frankl. Inst.-Eng. Appl. Math. 348 (1) (2011) 90–100, http://dx.doi.org/10.1016/j.jfranklin.2009.02.005.

[3] D. Purwanto, R. Mardiyanto, K. Arai, Electric wheelchair control with gaze direction and eye blinking, in: Proceedings of the 14th International Symposium on Artificial Life and Robotics, AROB, Oita, Japan, February 5–7, 2009, pp. 400–436, http://dx.doi.org/10.1007/s10015-009-0694-x.

[4] J.Y. Long, Y. Li, H. Wang, T. Yu, J. Pan, F. Li, A hybrid brain computer interface to control the direction and speed of a simulated or real wheelchair, IEEE Trans. Neural Syst. Rehabil. Eng. 20 (5) (2012) 720–729, http://dx.doi.org/10.1109/TNSRE.2012.2197221.

[5] R. Barea, L. Boquete, M. Mazo, E. Lopez, L.M. Bergasa, EOG guidance of a wheelchair using neural networks, in: 15th International Conference on Pattern Recognition, ICPR, vol. 4, Barcelona, Spain, 2000, pp. 668–671, http://dx.doi.org/10.1109/ICPR.2000.903006.

[6] A. Phinyomark, C. Limsakul, A review of control methods for electric power wheelchairs based on electromyography signals with special emphasis on pattern recognition, IETE Tech. Rev. 28 (4) (2011) 316–326, http://dx.doi.org/10.4103/0256-4602.83552.

[7] L.J. Hargrove, K. Englehart, B. Hudgins, A comparison of surface and intramuscular myoelectric signal classification, IEEE Trans. Biomed. Eng. (2007) 847–853, http://dx.doi.org/10.1109/TBME.2006.889192.

[8] T.R. Farrell, R.F. Weir, A comparison of the effects of electrode implantation and targeting on pattern classification accuracy for prosthesis control, IEEE Trans. Biomed. Eng. 55 (9) (2008) 2198–2211, http://dx.doi.org/10.1109/TBME.2008.923917.

[9] R.B. Stein, D. Charles, M. Walley, Bioelectric control of powered limbs for amputees, Adv. Neurol. 39 (1983) 1093–1108, ISSN: 6660094.

[10] F.R. Tucker, N. Peteleski, Microelectronic telemetry implant for myoelectric control of a powered prosthesis, Electr. Eng. J. 2 (4) (1977) 3–8, http://dx.doi.org/10.1109/CEEJ.1977.6593107.

[11] M. Santa-Cruz, R.R. Riso, F. Sepulveda, B. Lange, Natural control of wrist movements for myoelectric prostheses, in: Engineering in Medicine and Biology, 21st Annual Conference and the 1999 Annual Fall Meeting of the Biomedical Engineering Society, BMES/EMBS Conference, Proceedings of the First Joint, vol. 1, Atlanta, Georgia, USA, October 13–16, 1999, p. 642, http://dx.doi.org/10.1109/IEMBS.1999.802720.

[12] M.C. Santa-Cruz, R.R. Riso, F. Sepulveda, Evaluation of neural network parameters towards enhanced recognition of naturally evoked EMG for prosthetic hand grasp control, in: 5th Annual Conference of the International Functional Electrical Stimulation Society, 6th Triennial Conference Neural Prostheses: Motor Systems, Alborg, Denmark, June 18–24, 2000, pp. 436–439.

[13] M.C. Santa-Cruz, R.R. Riso, B. Lange, F. Sepulveda, Natural control of key grip and precision grip movements for a myoelectric prosthesis, in: MEC 99, Proceedings of the 1999 MyoElectric Controls/Powered Prosthetics Symposium Fredericton, New Brunswick, Canada, August, 1999, pp. 106–112.

[14] M.J.M. Hoozemans, J.H. Van Dieën, Prediction of handgrip forces using surface EMG of forearm muscles, J. Electromyogr. Kinesiol. 15 (4) (2005) 358–366, http://dx.doi.org/10.1016/j.jelekin.2004.09.001.

[15] M. Bilodeau, S. Schindler-Ivens, D.M. Williams, R. Chandran, S.S. Sharma, EMG frequency content changes with increasing force and during fatigue in the quadriceps femoris muscle of men and women, J. Electromyogr. Kinesiol. 1 (2003) 83–92, http://dx.doi.org/10.1016/S1050-6411(02)00050-0.

[16] R. Reiter, Eine neue elecktrokunsthand, Grenzgeb. Med. 4 (1948) 133–135.

[17] A.E. Kobrinski, S.V. Bolkovitin, L.M. Voskoboinikova, Problems of bioelectric control, in: J.F. Coles (Ed.), Proceedings 1st IFAC International Congress of Automatic and Remote Control, vol. 2, 1960, pp. 619–629.

[18] A.B. Ajiboye, R.F. Weir, A heuristic fuzzy logic approach to EMG pattern recognition for multifunctional prosthesis control, IEEE Trans. Neural Syst. Rehabil. Eng. 13 (3) (2005) 280–291, http://dx.doi.org/10.1109/TNSRE.2005.847357.

[19] C.N. Huang, C.H. Chen, H.Y. Chung, Application of facial electromyography in computer mouse access for people with disabilities, Disabil. Rehabil. 28 (4.) (2006) 231–237, http://dx.doi.org/10.1080/09638280500158349.

[20] D.P. Ferris, C.L. Lewis, Robotic lower limb exoskeletons using proportional myoelectric control, in: Annual International Conference of the IEEE Engineering in Medicine and Biology Society, EMBC, Minneapolis, MN, USA, September 3–6, 2009, pp. 2119–2124, http://dx.doi.org/10.1109/IEMBS.2009.5333984.

[21] S. Micera, J. Carpaneto, S. Raspopovic, Control of hand prostheses using peripheral information, IEEE Rev. Biomed. Eng. 3 (2010) 48–68, http://dx.doi.org/10.1109/RBME.2010.2085429.

[22] I. Moon, M. Lee, J. C.H.U., M. Mun, Wearable EMG-based HCI for electric-powered wheelchair users with motor disabilities, in: International Conference on Robotics and Automation, ICRA, April 18–22, Barcelona, Spain, 2005, pp. 2649–2654, http://dx.doi.org/10.1109/ROBOT.2005.1570513.

[23] C.E. Stepp, Surface electromyography for speech and swallowing systems: measurement, analysis, and interpretation (clinical report), J. Speech Lang. Hear. Res. 55 (4) (2012) 1232–1246, http://dx.doi.org/10.1044/1092-4388(2011/11-0214).

[24] X. Shusong, Z. Xia, EMG-driven computer game for post-stroke rehabilitation, in: IEEE Conference on Robotics Automation and Mechatronics, RAM, Singapore, 2010, pp. 32–36, http://dx.doi.org/10.1109/RAMECH.2010.5513218.

[25] E. Costanza, A. Perdomo, S.A. Inverso, R. Allen, EMG as a subtle input interface for mobile computing, in: 6th International Symposium, Mobile Human–Computer Interaction, MobileHCI 2004, vol.

3160, Glasgow, UK, September 13–16, 2004, pp. 426–430, http://dx.doi.org/10.1007/978-3-540-28637-0_50.
[26] E. Costanza, S.A. Inverso, R. Allen, P. Maes, Intimate interfaces in action: assessing the usability and subtlety of EMG-based motionless gestures, in: Proceedings of the SIGCHI Conference on Human Factors in Computing Systems, CHI '07, 2007, pp. 819–828, http://dx.doi.org/10.1145/1240624.1240747.
[27] E. Costanza, S.A. Inverso, R. Allen, Toward subtle intimate interfaces for mobile devices using an EMG controller, in: Proceedings of the SIGCHI Conference on Human Factors in Computing Systems, CHI '05, April 2–7, 2005, pp. 481–489, http://dx.doi.org/10.1145/1054972.1055039.
[28] C. Jorgensen, S. Dusan, Speech interfaces based upon surface electromyography, Speech Commun. 52 (4) (2010) 354–366, http://dx.doi.org/10.1016/j.specom.2009.11.003.
[29] T.S. Saponas, D.S. Tan, D. Morris, J. Tuner, J.A. Landay, Making muscle–computer interfaces more practical, in: Proceedings of the SIGCHI Conference on Human Factors in Computing Systems, CHI '10, 2010, pp. 851–854, http://dx.doi.org/10.1145/1753326.1753451.
[30] T.S. Saponas, D.S. Tan, D. Morris, R. Balakrishnan, Demonstrating the feasibility of using forearm electromyography for muscle–computer interfaces, in: Proceedings of the SIGCHI Conference Human Factors in Computing Systems, CHI '08, 2008, pp. 515–524, http://dx.doi.org/10.1145/1357054.1357138.
[31] Y.J. Joon, K.P. Yun, W.L. Jeun. Wearable mobile phone using EMG and controlling method thereof. U.S. Patent 2006/0121958, June 8, 2006.
[32] T. Desney, T.S. Saponas, D.M.J. Turner, Wearable electromyography-based controllers for human–computer interface. *US. Patent 8 170 656*, May 1, 2012.
[33] T. Finni, M. Hu, P. Kettunen, T. Vilavuo, S. Cheng, Measurement of EMG activity with textile electrodes embedded into clothing, Physiol. Meas. 28 (11) (2007) 1405–1419, http://dx.doi.org/10.1088/0967-3334/28/11/007.
[34] D. Farina, T. Lorrain, F. Negro, N. Jiang, High-density EMG e-textile systems for the control of active prostheses, in: 32nd Annual International Conference of the IEEE Engineering in Medicine and Biology Society (EMBC), Buenos Aires, Argentina, September 1–4, 2010, pp. 3591–3593, http://dx.doi.org/10.1109/IEMBS.2010.5627455.
[35] M. Barbero, R. Merletti, A. Rainoldi, Atlas of Muscle Innervation Zones, Springer-Verlag Italia, Milan, Italy, 2012, ISBN 978-88-470-2462-5.
[36] F.V.G. Tenore, A. Ramos, A. Fahmy, S. Acharya, R. etienne-Cummings, N.V. Thakor, Decoding of individuated finger movements using surface electromyography, IEEE Trans. Biomed. Eng. 56 (5) (2009) 1427–1434, http://dx.doi.org/10.1109/TBME.2008.2005485.
[37] H. He, K. Kiguchi, A Study on EMG-based control of exoskeleton robots for human lower-limb motion assist, in: 6th International Special Topic Conference on Information Technology Applications in Biomedicine, ITAB 2007, Tokyo, Japan, November 8–11, 2007, pp. 292–295, http://dx.doi.org/10.1109/ITAB.2007.4407405.
[38] J. Szu-Chen, L. Maier-Hein, T. Schultz, A. Waibel, Articulatory feature classification using surface electromyography, in: 2006 IEEE International Conference on Acoustics, Speech and Signal Processing, ICASSP 2006 Proceedings, Toulouse, France, May 14–19, 2006, pp. 292–295, http://dx.doi.org/10.1109/ICASSP.2006.1660093.
[39] N. Sugie, K. Tsunoda, A speech prosthesis employing a speech synthesizer-vowel discrimination from perioral muscle activities and vowel production, IEEE Trans. Biomed. Eng. 32 (1985) 485–490, http://dx.doi.org/10.1109/TBME.1985.325564.
[40] M. Wand, T. Schultz, Analysis of phone confusion in EMG-based speech recognition, in: 2011 IEEE International Conference on Acoustics, Speech and Signal Processing, ICASSP, Prague, Czech Republic, 2011, pp. 757–760, http://dx.doi.org/10.1109/ICASSP.2011.5946514.
[41] F.C.P. Sebelius, B.N. Rosén, G.N. Lundborg, Refined myoelectric control in below-elbow amputees using artificial neural networks and data glove, J. Hand Surg.-Am. 30A (4) (2005) 780–789, http://dx.doi.org/10.1016/j.jhsa.2005.01.002.
[42] G. Li, A.E. Schultz, T.A. Kuiken, Quantifying pattern recognition-based myoelectric control of multifunctional transradial prostheses, IEEE Trans. Neural Syst. Rehabil. Eng. 18 (2) (2010) 185–192, http://dx.doi.org/10.1109/TNSRE.2009.2039619.
[43] M.A. Oskoei, H. Hu, Myoelectric control systems – a survey, Biomed. Signal Process. Control (2007) 275–294, http://dx.doi.org/10.1016/j.bspc.2007.07.009.
[44] R. Merletti, M. Aventaggiato, A. Botter, A. Holobar, H. Marateb, T.M. Vieira, Advances in surface EMG: recent progress in detection and processing techniques, Crit. Rev. Biomed. Eng. 38 (4) (2010) 305–345, http://dx.doi.org/10.1615/CritRevBiomedEng.v38.i4.10.
[45] R. Merletti, P. Parker, Electromyography: Physiology, Engineering, and Non-Invasive Applications, Wiley-IEEE Press, 2004, August, ISBN 978-0-471-67580-8.
[46] R. Merletti, A. Bottera, A. Troianoa, E. Merloa, M.A. Minetto, Technology and instrumentation for detection and conditioning of the surface electromyographic signal: state of the art, Clin. Biomech. 24 (2) (2009) 122–134, http://dx.doi.org/10.1016/j.clinbiomech.2008.08.006.
[47] H.J. Hermens, B. Freriks, C. Disselhorst-KLUG, G. Rau, Development of recommendations for sEMG sensors and sensor placement procedures, J. Electromyogr. Kinesiol. 10 (5) (2000) 361–374, http://dx.doi.org/10.1016/S1050-6411(00)00027-4.
[48] Y. Fukuoka, K. Miyazawa, H. Mori, M. Miyagi, M. Nishida, Y. Horiuchi, A. Ichikawa, H. Hoshino, M. Noshiro, A. Ueno, Development of a compact wireless Laplacian electrode module for electromyograms and its human interface applications, Sensors 13 (2) (2013) 2368–2383, http://dx.doi.org/10.3390/s130202368.
[49] A. Ueno, Y. Uchikawa, M. Noshiro, A capacitive sensor system for measuring Laplacian electromyogram through cloth: a pilot study, in: 29th Annual International Conference of the IEEE Engineering in Medicine and Biology Society, EMBS 2007, Lyon, France, August 22–26, 2007, pp. 5731–5734, http://dx.doi.org/10.1109/IEMBS.2007.4353648.
[50] A. Boschmann, M. Platzner, Reducing the limb position effect in pattern recognition based myoelectric control using a high density electrode array, in: Biosignals and Biorobotics Conference, BRC, Rio de Janeiro, Brazil, February 18–20, 2013, pp. 1–5, http://dx.doi.org/10.1109/BRC.2013.6487548.
[51] A. Boschmann, M. Platzner, Reducing classification accuracy degradation of pattern recognition based myoelectric control caused by electrode shift using a high density electrode array, in: Annual International Conference of the IEEE Engineering in Medicine and Biology Society, EMBC 2012, San Diego, CA, USA, August 28–September 1, 2012, pp. 4324–4327, http://dx.doi.org/10.1109/EMBC.2012.6346923.
[52] Seniam. Sensor Placements Available from: http://www.seniam.org/
[53] H.W. Tam, J.G. Webster, Minimizing electrode motion artifact by skin abrasion, IEEE Trans. Bio-med. Eng. 24 (2) (1977) 134–139, http://dx.doi.org/10.1109/TBME.1977.326117.
[54] A. Searle, L.A. Kirkup, Direct comparison of wet, dry and insulating bioelectric recording electrodes, Physiol. Meas. 21 (2) (2000) 271–283, http://dx.doi.org/10.1088/0967-3334/21/2/307.
[55] P. Laferriere, A.D.C. Chan, E.D. Lemaire, Surface electromyographic signals using a dry electrode, in: Medical Measurements and Applications Proceedings, MeMeA, April 30–May 1, 2010, pp. 77–80, http://dx.doi.org/10.1109/MEMEA.2010.5480213.
[56] M.R. Neuman, Biopotential electrodes, in: J.G. Webster (Ed.), Medical Instrumentation: Application and Design, 3rd ed., John Wiley & Sons, Inc., New York, 1998, pp. 183–232.
[57] C. Pylatiuk, M. Mueller-Riederer, A. Kargov, S. Schulz, O. Schill, M. Reischl, G. Bretthauer, Comparison of surface EMG monitoring electrodes for long-term use in rehabilitation device control, in: IEEE 11th International Conference on Rehabilitation Robotics, vols. 1 and 2, ICORR, Kyoto, Japan, June 23–26, 2009, pp. 348–352, http://dx.doi.org/10.1109/ICORR.2009.5209576.
[58] A.J. Young, L.J. Hargrove, T.A. Kuiken, The effects of electrode size and orientation on the sensitivity of myoelectric pattern recognition systems to electrode shift, IEEE Trans. Biomed. Eng. (2011) 2537–2544, http://dx.doi.org/10.1109/TBME.2011.2159216.
[59] L. Hargrove, N.B. Fredericton, K. Englehart, B. Hudgins, The effect of electrode displacements on pattern recognition based myoelectric control, in: EMBS '06, 28th Annual International Conference of the IEEE Engineering in Medicine and Biology Society, New York, NY, USA, August 30–September 3, 2006, pp. 2203–2206, http://dx.doi.org/10.1109/IEMBS.2006.260681.
[60] L. Hargrove, K. Englehart, B. Hudgins, A Training Strategy to reduce classification degradation due to electrode displacements in pattern recognition based myoelectric control, Biomed. Signal Process. Control 3 (April (2)) (2008) 175–180, http://dx.doi.org/10.1016/j.bspc.2007.11.005.
[61] D.F. Stegeman, H.J. Hermens, Standards for surface electromyography, in: The European Project Surface EMG for Non-Invasive Assessment of Muscles (SENIAM), 2007.
[62] D. Farina, R. Merletti, Effect of electrode shape on spectral features of surface detected motor unit action potentials, Acta Physiol. Pharmacol. Bulg. 26 (1–2) (2001) 63, ISSN: 0323-9950.
[63] D. Farina, C. Cescon, R. Merletti, Influence of anatomical, physical, and detection-system parameters on surface EMG, Biol. Cybern. 86 (6) (2002) 445–456, http://dx.doi.org/10.1007/s00422-002-0309-2.
[64] Young, J. Aaron, L.J. Hargrove, T.A. Kuiken, Improving myoelectric pattern recognition robustness to electrode shift by changing interelectrode distance and electrode configuration, IEEE Trans. Biomed. Eng. 59 (3) (2012) 645–652, http://dx.doi.org/10.1109/TBME.2011.2177662.
[65] D. Farina, C. Cescon, Concentric-ring electrode systems for noninvasive detection of single motor unit activity, IEEE Trans. Biomed. Eng. 48 (11) (2001) 1326–1334, http://dx.doi.org/10.1109/10.959328.
[66] B. Afsharipour, K. Ullah, R. Merletti, Spatial aliasing and EMG amplitude in time and space: simulated action potential maps, in: XIII Mediterranean Conference on Medical and Biolagical Engineering and Computing 2013. IFMBE Proceedings, vol. 41, Seville, Spain, 2014, pp. 293–296, http://dx.doi.org/10.1007/978-3-319-00846-2_73.
[67] K. Saitou, T. Masuda, D. Michikami, R. Kojima, M. Okada, Innervation zones of the upper and lower limb muscles estimated by using multichannel surface EMG, J. Hum. Ergol. (Tokyo) 29 (1–2) (2000) 35–52, ISSN: 0300-8134.
[68] R. Merletti, P. Parker, H.J. Hermens, Detection and conditioning of the surface EMG signal, Electromyogr.: Physiol. Eng. Non-Invasive Appl. (2004) 107, http://dx.doi.org/10.1002/0471678384.ch5.
[69] D. Falla, P. Dall'alba, A. Rainoldi, R. Merletti, G. Jull, Location of innervation zones of sternocleidomastoid and scalene muscles – a basis for clinical and research electromyography applications, Clin. Neurophysiol. 113 (1) (2002) 57–63, http://dx.doi.org/10.1016/S1388-2457(01)00708-8.
[70] T. Castroflorio, D. Farina, A. Bottin, C. Debernardi, P. Bracco, R. Merletti, G. Anastasi, P. Bramanti, Non-invasive assessment of motor unit anatomy in jaw-elevator muscles, J. Oral Rehabil. 32 (10) (2005) 708–713, http://dx.doi.org/10.1111/j.1365-2842.2005.01490.x.

[71] S. Martin, D. Macisaac, Innervation Zone shift with changes in joint angle in the brachial biceps, J. Electromyogr. Kinesiol. 16 (2) (2006) 144–148, http://dx.doi.org/10.1016/j.jelekin.2005.06.010.
[72] H. Piitulainen, T. Rantalainen, V. Linnamo, P. Komi, J. Avela, Innervation zone shift at different levels of isometric contraction in the biceps brachii muscle, J. Electromyogr. Kinesiol. 19 (4) (2009) 667–675, http://dx.doi.org/10.1016/j.jelekin.2008.02.007.
[73] J.A. Hodgson, T. Finni, A.M. Lai, V.R. Edgerton, S. Sinha, Influence of structure on the tissue dynamics of the human soleus muscle observed in MRI studies during isometric contractions, J. Morphol. 267 (5) (2006) 584–601, http://dx.doi.org/10.1002/jmor.10421.
[74] B. Hudgins, P. Parker, R.N. Scott, A New strategy for multifunction myoelectric control, IEEE Trans. Biomed. Eng. 40 (1) (1993) 82–94, http://dx.doi.org/10.1109/10.204774.
[75] M. Rojas-Martinez, M.A. Mananas, J.F. Alonso, High-density surface EMG maps from upper-arm and forearm muscles, J. NeuroEng. Rehabil. – JNER 9 (1) (2012) 1–17, http://dx.doi.org/10.1186/1743-0003-9-85.
[76] A. Stango, F. Negro, D. Farina, Spatial correlation of high density EMG signals provides features robust to electrode number and shift in pattern recognition for myocontrol, IEEE Trans. Neural Syst. Rehabil. Eng. (2014), http://dx.doi.org/10.1109/TNSRE.2014.2366752.
[77] N. Ostlund, B. Gerdle, J. Stefan Karlsson, Location of innervation zone determined with multichannel surface electromyography using an optical flow technique, J. Electromyogr. Kinesiol.: Off. J. Int. Soc. Electrophysiol. Kinesiol. 17 (5) (2007) 549–555, http://dx.doi.org/10.1016/j.jelekin.2006.06.002.
[78] A. Andrews, E. Morin, L. Mclean, Optimal electrode configurations for finger movement classification using EMG, in: 31st Annual International Conference of the IEEE EMBS, Minneapolis, Minnesota, USA, September 2–6, 2009, pp. 2987–2990, http://dx.doi.org/10.1109/IEMBS.2009.5332520.
[79] A.J. Andrews, Finger Movement Classification using Forearm EMG Signals (MS thesis), October 31, Queen's University, Kingston, Ontario, Canada, 2008, Available from: https://qspace.library.queensu.ca/handle/1974/1574
[80] H. Marateb, M. Rojas-Martinez, M. Mansourian, R. Merletti, M. Mananas-Villanueva, Outlier detection in high-density surface electromyographic signals, Med. Biol. Eng. Comput. 50 (1) (2012) 79–89, http://dx.doi.org/10.1007/s11517-011-0790-7.
[81] G. Li, Y. Li, L. Yu, Y. Geng, Conditioning and sampling issues of EMG signals in motion recognition of multifunctional myoelectric prostheses, Ann. Biomed. Eng. 39 (6) (2011) 1779–1787, http://dx.doi.org/10.1007/s10439-011-0265-x.
[82] G. Li, Y. Li, Z. Zhang, Y. Geng, R. Zhou, Selection of sampling rate for EMG pattern recognition based prosthesis control, in: Annual International Conference of the IEEE Engineering in Medicine and Biology Society (EMBC), Buenos Aires, Argentina, August 31–September 4, 2010, pp. 5058–5061, http://dx.doi.org/10.1109/IEMBS.2010.5626224.
[83] E.A. Clancy, L.E. Morin, R. Merletti, Sampling, noise reduction and amplitude estimation issues in surface electromyography, J. Electromyogr. Kinesiol. 12 (1) (2002) 1–16, http://dx.doi.org/10.1016/S1050-6411(01)00033-5.
[84] K. Das, Z. Nenadic, An efficient discriminate-based solution for small sample size problem, Pattern Recognit. 42 (2008) 857–866, http://dx.doi.org/10.1016/j.patcog.2008.08.036.
[85] L. Hargrove, E. Scheme, K. Englehart, B. Hudgins, Principal component analysis preprocessing to reduce controller delays in pattern recognition based myoelectric control, in: Annual International Conference of the IEEE Engineering in Medicine and Biology – Proceedings, Lyon, France, August 22–26, 2007, pp. 6512–6515, http://dx.doi.org/10.1109/IEMBS.2007.4353851.
[86] L.J. Hargrove, G. Li, K. Englehart, B. Hudgins, Principal components analysis preprocessing for improved classification accuracies in pattern-recognition-based myoelectric control, IEEE Trans. Biomed. Eng. 56 (5) (2009) 1407–1414, http://dx.doi.org/10.1109/TBME.2008.2008171.
[87] A. Hyvärinen, E. Oja, Independent Component Analysis: A Tutorial, Helsinki University of Technology. Laboratory of Computer and Information Science, Espoo, Finland, 2000, Available from: http://cis.legacy.ics.tkk.fi/aapo/papers/IJCNN99_tutorialweb/IJCNN99_tutorial3.html (accessed 19.04.2000).
[88] G. Naik, A comparison of ICA algorithms in surface EMG signal processing, Int. J. Biomed. Eng. Technol. 6 (7) (2011) 363–374, http://dx.doi.org/10.1504/IJBET.2011.041774.
[89] A.H. Al-Timemy, G. Bugmann, N. Outram, J. Escudero, Reduction in classification errors for myoelectric control of hand movements with independent component analysis, in: The 5th International Conference on Information Technology, ICIT 2011, 2011.
[90] D. Nishikawa, W. Yu, H. Yokoi, Y. Kakazu, On-line supervising mechanism for learning data in surface electromyogram motion classifiers, Syst. Comput. Jpn. 33 (14) (2002) 1–11, http://dx.doi.org/10.1002/scj.10245.
[91] T.R. Farrell, Determining delay created by multifunctional prosthesis controllers, J. Rehabil. Res. Dev. 48 (6) (2011) xxi–xxxviii, http://dx.doi.org/10.1682/JRRD.2011.03.0055.
[92] K. Englehart, B. Hudgins, A robust, real-time control scheme for multifunction myoelectric control, IEEE Trans. Biomed. Eng. 50 (7) (2003) 848–854, http://dx.doi.org/10.1109/TBME.2003.813539.
[93] M.A. Oskoei, H. Hu, Support vector machine-based classification scheme for myoelectric control applied to upper limb, IEEE Trans. Biomed. Eng. 55 (8) (2008) 1956–1965, http://dx.doi.org/10.1109/TBME.2008.919734.
[94] T.R. Farrell, R.F. Weir, The optimal controller delay for myoelectric prostheses, IEEE Trans. Neural Syst. Rehabil. Eng. 15 (1) (2007) 111–118, http://dx.doi.org/10.1109/TNSRE.2007.891391.
[95] K. Englehart, B. Hudgins, A. Chan, Continuous multifunction myoelectric control using pattern recognition, Technol. Disabil. (2003) 95–103, ISSN: 1055-4181.
[96] W. Hefftner, W. Zucchini, G.G. Jaros, The electromyogram (EMG) as a control signal for functional neuromuscular stimulation—Part I: Autoregressive modeling as a means of EMG signature discrimination, IEEE Trans. Biomed. Eng. 35 (4) (1988) 230–237, http://dx.doi.org/10.1109/10.1370.
[97] J. Graupe, J. Salahi, D. Zhang, Stochastic analysis of electromyogram temporal signatures for multifunctional signal-site activation of prostheses and orthoses, J. Biomed. Eng. (1985) 18–29, http://dx.doi.org/10.1016/0141-5425(85)90004-4.
[98] J.-U. Chu, I. Moon, M.S. Mun, A real-time EMG pattern recognition system based on linear–nonlinear feature projection for a multifunction myoelectric hand, IEEE Trans. Biomed. Eng. 53 (11) (2006) 2232–2239, http://dx.doi.org/10.1109/TBME.2006.883695.
[99] D. Graupe, J. Salahi, K.H. Kohn, Multifunctional prosthesis and orthosis control via microcomputer identification of temporal pattern differences in single-site myoelectric signals, J. Biomed. Eng. 4 (1982) 17–22, http://dx.doi.org/10.1016/0141-5425(82)90021-8.
[100] K. Englehart, B. Hudgins, P.A. Parker, A wavelet-based continuous classification scheme for multifunction myoelectric control, IEEE Trans. Biomed. Eng. 48 (3) (2001) 302–310, http://dx.doi.org/10.1109/10.914793.
[101] S.C. Gandevia, Spinal and supraspinal factors in human muscle fatigue, Physiol. Rev. 81 (4) (2001) 1725–1789, ISSN: 00319333.
[102] N.K. Vollestad, Measurement of human muscle fatigue, J. Neurosci. Methods 74 (2) (1997) 219–227, ISSN: 0165-0270.
[103] C. Jun-Uk, M. Inhyuk, L. Yun-Jung, K. Shin-Ki, M. Mu-Seong, A supervised feature-projection-based real-time EMG pattern recognition for multifunction myoelectric hand control, IEEE/ASME Trans. Mechatron. 12 (3) (2007) 282–290, http://dx.doi.org/10.1109/TMECH.2007.897262.
[104] T. Lorrain, N. Jiang, D. Farina, Influence of the training set on the accuracy of surface EMG classification in dynamic contractions for the control of multifunction prostheses, J. Neuroeng. Rehabil. 8 (25) (2011), http://dx.doi.org/10.1186/1743-0003-8-25.
[105] T. Kiryu, M. Morishiata, H. Yamada, M. Okada, A muscular fatigue index based on the relationships between superimposed m wave and preceding background activity, IEEE Trans. Biomed. Eng. 45 (10) (1998) 1194–1204, http://dx.doi.org/10.1109/10.720197.
[106] R. Merletti, S. Roy, Myoelectric and mechanical manifestations of muscle fatigue in voluntary contractions, J. Orthop. Sports Phys. Therapy 24 (6) (1996) 342–353.
[107] A. Kiso, S. Hirokazu, Discrimination of human forearm motions on the basis of myoelectric signals by using adaptive fuzzy inference system, IEEJ Trans. Ind. Appl. 130 (11) (2010) 1272–1278, http://dx.doi.org/10.1541/ieejias.130.1272.
[108] K. Ishikawa, M. Toda, S. Sakurazawa, J. Akita, K. Kondo, Y. Nakamura, Robust finger motion classification using frequency characteristics of surface electromyogram signals, in: International Conference on Biomedical Engineering, ICoBE, Penang, Malaysia, February 27–28, 2012, pp. 362–367, http://dx.doi.org/10.1109/ICoBE.2012.6179039.
[109] A. Phinyomark, P. Phukpattaranont, C. Limsakul, Feature reduction and selection for EMG signal classification, Expert Syst. Appl. 39 (8) (2012) 7420–7431, http://dx.doi.org/10.1016/j.eswa.2012.01.102.
[110] R. Boostani, M.H. Moradi, Evaluation of the forearm EMG signal features for the control of a prosthetic hand, Physiol. Meas. 24 (2) (2003) 309–319, http://dx.doi.org/10.1088/0967-3334/24/2/307.
[111] M. Zardoshti-Kermani, B.C. Wheeler, K. Badie, R.M. Hashemi, EMG feature evaluation for movement control of upper extremity prostheses, IEEE Trans. Rehabil. Eng. (1995) 324–333, http://dx.doi.org/10.1109/86.481972.
[112] S.H. Park, S.P. Lee, EMG pattern recognition based on artificial intelligence techniques, IEEE Trans. Rehabil. Eng. 6 (4) (1998) 400–405, http://dx.doi.org/10.1109/86.736154.
[113] Y.C. Du, C.H. Linb, L.Y. Shyuc, T. Chen, Portable hand motion classifier for multi-channel surface electromyography recognition using grey relational analysis, Expert Syst. Appl. 37 (6) (2010) 4283–4291, http://dx.doi.org/10.1016/j.eswa.2009.11.072.
[114] K.S. Kim, H.H. Choi, C.S. Moon, W.H. Muna, Comparison of *k*-nearest neighbor, quadratic discriminate and linear discriminate analysis in classification of electromyogram signals based on the wrist-motion directions, Curr. Appl. Phys. 11 (3) (2010) 740–745, http://dx.doi.org/10.1016/j.cap.2010.11.051.
[115] D. Tkach, H. Huang, T.A. Kuiken, Study of stability of time-domain features for electromyographic pattern recognition, J. NeuroEng. Rehabil. 7 (21.) (2010), http://dx.doi.org/10.1186/1743-0003-7-21.
[116] G.C. Chang, W.J. Kang, J.J. Luh, C.K. Cheng, J.S. Lai, J.J. Chen, T.S. Kuo, Real-time implementation of electromyogram pattern recognition as a control command of man–machine interface, Med. Eng. Phys. 18 (7) (1996) 529–537, http://dx.doi.org/10.1016/1350-4533(96)00006-9.
[117] F. Tenore, A. Ramos, A. Fahmy, S. Acharya, R. Etienne-Cummings, N.V. Thakor, Towards the control of individual fingers of a prosthetic hand using surface EMG signals, in: Engineering in Medicine and Biology Society, 2007. EMBS 2007. 29th Annual International Conference of the IEEE, Lyon, France, August 22–26, 2007, pp. 6145–6149, http://dx.doi.org/10.1109/IEMBS.2007.4353752.

[118] M. Zecca, S. Micera, M.C. Carrozza, P. Dario, Control of multifunctional prosthetic hands by processing the electromyographic signal, Crit. Rev. Biomed. Eng. 30 (4–6) (2002) 459–485, http://dx.doi.org/10.1615/CritRevBiomedEng.v30.i456.80.
[119] Y.-H. Liu, H.-P. Huang, C.-H. Weng, Recognition of electromyographic signals using cascaded kernel learning machine, IEEE/ASME Trans. Mechatron. 12 (3) (2007) 253–264, http://dx.doi.org/10.1109/TMECH.2007.897253.
[120] P. Phinyomark, S. Thongpanja, H. Hu, P. Phukpattaranont, C. Limsakul, The usefulness of mean and median frequencies in electromyography analysis, in: R.G. Naik (Ed.), Computational Intelligence in Electromyography Analysis – A Perspective on Current Applications and Future Challenges, InTech, 2012, ISBN 978-953-51-0805-4, pp. 220–295, http://dx.doi.org/10.5772/50639, Available from: http://www.intechopen.com/books/computational-intelligence-in-electromyography-analysis-a-perspective-on-current-applications-and-future-challenges/the-usefulness-of-mean-and-median-frequencies-in-electromyography-analysis
[121] A. Phinyomark, C. Limsakul, P. Phukpattaranont, A novel feature extraction for robust EMG pattern recognition, J. Comput. 1 (1) (2009 Dec.) 71–80, ISSN: 2151-9617.
[122] K. Englehart, B. Hudgins, P.A. Parker, M. Stevenson, Classification of the myoelectric signal using time-frequency based representations, Med. Eng. Phys. 21 (6–7) (1999) 431–438, ISSN:1350-4533.
[123] J. Zhao, Z. Xie, L. Jiang, H. Cai, H. Liu, G. Hirzinger, A five-fingered underactuated prosthetic hand control scheme, in: The First IEEE/RAS-EMBS International Conference on Biomedical Robotics and Biomechatronics, BioRob 2006, Pisa, Italy, February 20–22, 2006, pp. 995–1000, http://dx.doi.org/10.1109/BIOROB.2006.1639221.
[124] X. Zhang, Y. Yang, X. Xu, M. Zhang, Wavelet based neuro-fuzzy classification for EMG control, in: IEEE 2002 International Conference on Communications, Circuits and Systems and West Sino Expositions, Chengdu, China, June 29–July 1, vol. 2, 2002, pp. 1087–1089, http://dx.doi.org/10.1109/ICCCAS.2002.1178974.
[125] Y. Huang, K.B. Englehart, B. Hudgins, A.D.C. Chan, A Gaussian mixture model based classification scheme for myoelectric control of powered upper limb prostheses, IEEE Trans. Biomed. Eng. (2005) 1801–1811, http://dx.doi.org/10.1109/TBME.2005.856295.
[126] E. Scheme, K. Englehart, B. Hudgins, A one-versus-one classifier for improved robustness of myoelectric control, in: The 18th Congress of the International Society of Electrophysiology and Kinesiology, Aalborg, Denmark, 2010.
[127] A. Phinyomark, S. Hirunviriya, C. Limsakul, P. Phukpattaranont, Evaluation of EMG feature extraction for hand movement recognition based on Euclidean distance and standard deviation, in: ECTI International Conference on Electrical Engineering/Electronics, Computer, Telecommunications and Information Technology, ECTI-CON, Chiang Mai, Thailand, May 19–21, 2010, ISBN 9789746724913, pp. 856–860.
[128] M.A. Oskoei, H. Hu, GA-based feature subset selection for myoelectric classification, in: International Conference on Robotics and Biomimetics, Kuming, China, December 17–20, 2006, pp. 1465–1470, http://dx.doi.org/10.1109/ROBIO.2006.340145.
[129] A. Phinyomark, P. Phukpattaranont, C. Limsakul, Investigating long-term effects of feature extraction methods for continuous EMG pattern classification, Fluct. Noise Lett. 11 (4.) (2012), http://dx.doi.org/10.1142/S0219477512500289.
[130] A. Phinyomark, F. Quaine, S. Charbonnier, C. Serviere, F. Tarpin-Bernard, Y. Laurillau, EMG feature evaluation for improving myoelectric pattern recognition robustness, Expert Syst. Appl. 40 (12) (2013) 4832–4840, http://dx.doi.org/10.1016/j.eswa.2013.02.023.
[131] F.D. Farfan, J.C. Politti, C.J. Felice, Evaluation of EMG processing techniques using information theory, Biomed. Eng. Online 9 (2010), http://dx.doi.org/10.1186/1475-925X-9-72.
[132] X. Liu, R. Zhou, L. Yang, G. Li, Performance of various EMG features in identifying arm movements for control of multifunctional prostheses, in: IEEE Youth Conference on Information, Computing and Telecommunication, 2009, YC-ICT '09, Beijing, China, September 20–21, 2009, pp. 287–290, http://dx.doi.org/10.1109/YCICT.2009.5382366.
[133] A. Phinyomark, A. Nuidod, P. Phukpattaranont, C. Limsakul, Feature extraction and reduction of wavelet transform coefficients for EMG pattern classification, Electr. Eng. 122 (6) (2012) 27–32, http://dx.doi.org/10.5755/j01.eee.122.6.1816.
[134] F.H.Y. Chan, Y. Yong-Sheng, F.K. Lam, Z. Yuan-Ting, P.A. Parker, Fuzzy EMG classification for prosthesis control, IEEE Trans. Rehabil. Eng. (2000) 305–311, http://dx.doi.org/10.1109/86.867872.
[135] L. Philipson, The electromyographic signal used for control of upper extremity prostheses and for quantification of motor blockade during epidural anaesthesia (Dissertations), Linköping Studies in Science and Technology, 1987, ISBN 91-7870-228-3, ISSN: 0345-7524.
[136] M. Yoshikawa, M. Mikawa, K. Tanaka, A myoelectric interface for robotic hand control using support vector machine, in: IEEE/RSJ International Conference on Intelligent Robots and Systems, IROS 2007, San Diego, CA, USA, October 29–November 2, 2007, pp. 2723–2728, http://dx.doi.org/10.1109/IROS.2007.4399301.
[137] N. Jiang, J.L. Vest-Nielsen, S. Muceli, D. Farina, EMG-based simultaneous and proportional estimation of wrist/hand kinematics in unilateral transradial amputees, J. NeuroEng. Rehabil. – JNER 9 (1) (2012) 42–52, http://dx.doi.org/10.1186/1743-0003-9-42.
[138] T.R. Farrell, R.F. Weir, Pilot comparison of surface vs. implanted EMG for multifunctional prosthesis control, in: Proceedings of the 2005 IEEE 9th International Conference on Rehabilitation Robotics, ICORR, IL, Chicago, June 28–July 1, 2005, pp. 277–280, http://dx.doi.org/10.1109/ICORR.2005.1501101.
[139] D. Graupe, W.K. Cline, Functional separation of EMG signals via ARMA identification methods for prosthesis control purposes, IEEE Trans. Syst. Man Cybern. 5 (1975) 252–259, http://dx.doi.org/10.1109/TSMC.1975.5408479.
[140] F. Ayachi, S. Boudaoud, C. Marque, Evaluation of muscle force classification using shape analysis of the sEMG probability density function: a simulation study, Med. Biol. Eng. Comput. 52 (8) (2014) 673–684, http://dx.doi.org/10.1007/s11517-014-1170-x.
[141] M.R. Al-Mulla, F. Sepulveda, M. Colley, sEMG techniques to detect and predict localised muscle fatigue, in: M. Schwartz (Ed.), EMG Methods for Evaluating Muscle and Nerve Function, InTech, 2012, pp. 157–186, http://dx.doi.org/10.5772/25678.
[142] M. Cifrek, V. Medved, S. Tonković, S. Ostojić, Surface EMG-based muscle fatigue evaluation in biomechanics, Clin. Biomech. 24 (4) (2009) 327–340, http://dx.doi.org/10.1016/j.clinbiomech.2009.01.010.
[143] M.C.A. Santos, T.A. Semeghuini, F.M. De Azevedo, D.B. Colugnati, R.D. Negrao, N. Alves, R.M. Arida, Analysis of localized muscular fatigue in athletes and sedentary subjects through frequency parameters of electromyographic signal, Rev. Bras. Med. Esp. 14 (6) (2008) 509–512, ISSN: 1517-8692.
[144] L. Lindström, R. Kadefors, I. Petersén, An electromyographic index for localized muscle fatigue, J. Appl. Physiol.: Respir. Environ. Exerc. Physiol. 43 (4) (1977) 750–754, ISSN: 01617567.
[145] B. Bigland-Ritchie, EMG/force relations and fatigue of human voluntary contractions, Exerc. Sport Sci. Rev. 9 (1981) 75–117, http://dx.doi.org/10.1249/00003677-198101000-00002.
[146] D. Farina, R. Merletti, Comparison of algorithms for estimation of EMG variables during voluntary isometric contractions, J. Electromyogr. Kinesiol. 10 (5) (2000) 337–349, http://dx.doi.org/10.1016/S1050-6411(00)00025-0.
[147] S. Karlsson, J. Akay, Enhancement of spectral analysis of myoelectric signals during static contractions using wavelet methods, IEEE Trans. Rehabil. Eng. 46 (6) (1999) 670–684, http://dx.doi.org/10.1109/10.764944.
[148] J. He, D. Zhang, X. Sheng, S. Li, X. Zhu, Invariant surface EMG feature against varying contraction level for myoelectric control based on muscle coordination, IEEE J. Biomed. Health Inform. (2014), http://dx.doi.org/10.1109/JBHI.2014.2330356 (in press).
[149] Q. Zhang, Z. Luo, Wavelet de-noising of electromyography, in: International Conference on Mechatronics and Automation, Luoyang, Henan, China, June 25–28, 2006, pp. 1553–1558, http://dx.doi.org/10.1109/ICMA.2006.257406.
[150] A. Phinyomark, C. Limsakul, P. Phukpattaranont, Application of wavelet analysis in EMG feature extraction for pattern classification, Meas. Sci. Rev. 11 (2) (2011) 45–52, http://dx.doi.org/10.2478/v10048-011-0009-y.
[151] N.M. Kakoty, S.M. Hazarika, Recognition of grasp types through principal components of DWT-based EMG features, in: IEEE International Conference on Rehabilitation Robotics, ICORR, Luoyang, Henan, China, 2011, pp. 1–6, http://dx.doi.org/10.1109/ICORR.2011.5975398.
[152] M.-F. Lucas, A. Gaufriaua, S. Pascuala, C. Doncarlia, D. Farina, Multi-channel surface EMG classification using support vector machines and signal-based wavelet optimization, Biomed. Signal Process. Control 3 (2) (2008) 169–174, http://dx.doi.org/10.1016/j.bspc.2007.09.002.
[153] T.W. Beck, T.J. Housh, G.O. Johnson, J.P. Weir, J.T. Cramer, J.W. Coburn, M.H. Malek, Comparison of Fourier and wavelet transform procedures for examining the mechanomyographic and electromyographic frequency domain responses during fatiguing isokinetic muscle actions of the biceps brachii, J. Electromyogr. Kinesiol. 15 (2) (2005) 190–199, ISSN: 1050-6411.
[154] K. Xing, P. Yang, J. Huang, Y. Wang, Q. Zhu, A real-time EMG pattern recognition method for virtual myoelectric hand control, Neurocomputing 136 (2014) 345–355, http://dx.doi.org/10.1016/j.neucom.2013.12.010.
[155] A. Phinyomark, H. Hu, P. Phukpattaranont, C. Limsakul, Application of linear discriminate analysis in dimensionality reduction for hand motion classification, Meas. Sci. Rev. 12 (3) (2012) 82–89, http://dx.doi.org/10.2478/v10048-012-0015-8.
[156] A. Phinyomark, C. Limsakul, P. Phukpattaranont, A comparative study of wavelet denoising for multifunction myoelectric control, in: International Conference on Computer and Automation Engineering, ICCAE '09, Bangkok, Thailand, March 8–10, 2009, pp. 21–25, http://dx.doi.org/10.1109/ICCAE.2009.57.
[157] A. Phinyomark, C. Limsakul, P. Phukpattaranont, EMG denoising estimation based on adaptive wavelet thresholding for multifunction myoelectric control, in: Innovative Technologies in Intelligent Systems and Industrial Applications, CITISIA, Monash, July 25–26, 2009, pp. 171–176, http://dx.doi.org/10.1109/CITISIA.2009.5224220.
[158] A. Phinyomark, C. Limsakul, P. Phukpattaranont, An optimal wavelet function based on wavelet denoising for multifunction myoelectric control, in: 6th International Conference on Electrical Engineering/Electronics, Computer, Telecommunications and Information Technology, vol. 2, Pattaya, Chonburi, Thailand, May 6–9, 2009, pp. 1098–1101, http://dx.doi.org/10.1109/ECTICON.2009.5137236.
[159] F.A. Mahdavi, S.A. Ahmad, M.H. Marhaban, R. Mohammad, T. Akbarzadeh, The utility of wavelet transform in surface electromyography feature extraction – a comparative study of different mother wavelets, World Acad. Sci. Eng. Technol. Int. J. Electr. Robot. Electr. Commun. Eng. 7 (4) (2013) 57–62.

[160] A. Phinyomark, P. Phukpattaranont, C. Limsakul, Wavelet-based denoising algorithm for robust EMG pattern recognition, Fluct. Noise Lett. 10 (2) (2011) 157–167, http://dx.doi.org/10.1142/S0219477511000466.
[161] T.M.M. Vieira, R. Merletti, L. Mesin, Automatic segmentation of surface EMG images: improving the estimation of neuromuscular activity, J. Biomech. 43 (11) (2010) 2149–2158, http://dx.doi.org/10.1016/j.jbiomech.2010.03.049.
[162] K. Tucker, D. Falla, T. Graven-Nielsen, D. Farina, Electromyographic mapping of the erector spinae muscle with varying load and during sustained contraction, J. Electromyogr. Kinesiol. 19 (3) (2009) 373–379, http://dx.doi.org/10.1016/j.jelekin.2007.10.003.
[163] A. Holtermann, K. Roeleveld, J.S. Karlsson, Inhomogeneities in muscle activation reveal motor unit recruitment, J. Electromyogr. Kinesiol. 15 (2) (2005) 131–137, http://dx.doi.org/10.1016/j.jelekin.2004.09.003.
[164] R.R. Finley, R.W. Wirta, Myocoder studies of multiple myocoder response, Arch. Phys. Med. Rehabil. 48 (1967) 598–601, doi:6060789.
[165] J. Lyman, A. Freedy, R. Prior, Fundamental and applied research related to the design and development of upper-limb externally powered prostheses, Bull. Prosthet. Res. (1976) 184–195.
[166] J.M. Fontana, Classification of EMG signals to control a prosthetic hand using time-frequency representations and support vector machines (Dissertation), Louisiana Tech University, 2010, ISBN 9781124421360.
[167] M. Khezri, M. Jahed, N. Sadati, Neuro-fuzzy surface EMG pattern recognition for multifunctional hand prosthesis control, in: IEEE International Symposium on Industrial Electronics, Vigo, Spain, June 4–7, 2007, pp. 269–274, http://dx.doi.org/10.1109/ISIE.2007.4374610.
[168] K.-S. Lee, EMG-based speech recognition using hidden Markov models with global control variables (author abstract), IEEE Trans. Biomed. Eng. 55 (3) (2008), http://dx.doi.org/10.1109/TBME.2008.915658, p. 930(11), pp. 930–940.
[169] X. Yang, G. Zhang, J. LU, J. Ma, A Kernel fuzzy c-means clustering-based fuzzy support vector machine algorithm for classification problems with outliers or noises, IEEE Trans. Fuzzy Syst. 19 (1) (2011) 105–115, http://dx.doi.org/10.1109/TFUZZ.2010.2087382.
[170] E.J. Scheme, K.B. Englehart, B.S. Hudgins, Selective classification for improved robustness of myoelectric control under non-ideal conditions, IEEE Trans. Biomed. Eng. 58 (6) (2011) 1698–1705, http://dx.doi.org/10.1109/TBME.2011.2113182.
[171] D. Zhang, A. Xiong, X. Zhao, J. Han, PCA and LDA for EMG-based control of bionic mechanical hand, in: International Conference on Information and Automation, ICIA, Shenyang, China, June 6–8, 2012, pp. 960–965, http://dx.doi.org/10.1109/ICInfA.2012.6246955.
[172] L. Chen, Y. Geng, G. Li, Effect of upper-limb positions on motion pattern recognition using electromyography, in: 4th International Congress on Image and Signal Processing, CISP, vol. 1, Shanghai, China, October 15–17, 2011, pp. 139–142, http://dx.doi.org/10.1109/CISP.2011.6100025.
[173] E. Scheme, A. Fougner, Ø. Stavdahl, A.D.C. Chan, K. Englehart, Examining the adverse effects of limb position on pattern recognition based myoelectric control, in: Annual International Conference of the IEEE Engineering in Medicine and Biology Society, EMBC, Buenos Aires, Argentina, August 31–September 4, 2010, pp. 6337–6340, http://dx.doi.org/10.1109/IEMBS.2010.5627638.
[174] A. Young, L. Smith, E. Rouse, L. Hargrove, Classification of simultaneous movements using surface EMG pattern recognition, IEEE Trans. Biomed. Eng. 60 (5) (2013) 1250–1258, http://dx.doi.org/10.1109/TBME.2012.2232293.
[175] M.S. Erkilinc, F. Sahin, Camera control with EMG signals using principal component analysis and support vector machines, in: 2011 IEEE International Systems Conference, SysCon, Montreal, QC, Canada, April 4–7, 2011, pp. 417–421, http://dx.doi.org/10.1109/SYSCON.2011.5929070.
[176] A.D.C. Chan, K.B. Englehart, Continuous myoelectric control for powered prostheses using hidden Markov models, IEEE Trans. Biomed. Eng. 52 (1) (2005) 121–124, http://dx.doi.org/10.1109/TBME.2004.836492.
[177] E. Scheme, K.B. Englehart, Electromyogram pattern recognition for control of powered upper-limb prostheses: state of the art and challenges for clinical use, J. Rehabil. Res. Dev. 48 (6) (2011) 643–660, http://dx.doi.org/10.1682/JRRD.2010.09.0177.
[178] P. Kaufmann, K. Englehart, M. Platzner, Fluctuating EMG signals: investigating long-term effects of pattern matching algorithms, in: Annual International Conference of the IEEE Engineering in Medicine and Biology Society, EMBC'10, Buenos Aires, Argentina, Aug. 31-Sep. 4, 2010, pp. 6357–6360, http://dx.doi.org/10.1109/IEMBS.2010.5627288.
[179] X. Zhang, X. Wang, B. Wang, T. Sugi, M. Nakamura, Meal assistance system operated by electromyogram (EMG) signals: movement onset detection with adaptive threshold, Int. J. Control Autom. Syst. 8 (2) (2010) 392–397, http://dx.doi.org/10.1007/s12555-010-0226-4.
[180] H.H. Sears, J. Shaperman, Proportional myoelectric hand control: an evaluation, Am. J. Phys. Med. Rehabil. 70 (1) (1991) 20–28, http://dx.doi.org/10.1097/00002060-199102000-00005.
[181] Q. Sun, Y. Sun, X. Ding, Z. Ma, Onset determination of muscle contraction in surface electromyography signals analysis, in: IEEE International Conference on Information Acquisition, June 27–July 3, 2005, pp. 3957–3962, http://dx.doi.org/10.1109/ICIA.2005.1635117.
[182] P. Bonato, T. D'alessio, M. Knaflitz, A statistical method for the measurement of muscle activation intervals from surface myoelectric signal during gait, IEEE Trans. Biomed. Eng. 45 (3) (1998) 287–299, http://dx.doi.org/10.1109/10.661154.
[183] L. Xu, A. Adler, An improved method for muscle activation detection during gait, in: Canadian Conference on Electrical and Computer Engineering, vol. 1, Ontarino, Canada, May 2–4, 2004, pp. 357–360, http://dx.doi.org/10.1109/CCECE.2004.1345029.
[184] M.C. Carozza, G. Cappiello, G. Stellin, F. Zaccone, F. Vecchi, S. Micera, P. Dario, On the development of a novel adaptive prosthetic hand with compliant joints: experimental platform and EMG control, in: IEEE/RSJ International Conference on Intelligent Robots and Systems, IROS 2005, Edmonton, AB, Canada, August 2–6, 2005, pp. 1271–1276, http://dx.doi.org/10.1109/IROS.2005.1545585.
[185] S. Herle, S. Man, G. Lazea, C. Marcu, P. Raica, R. Robotin, Hierarchical myoelectric control of a human upper limb prosthesis, in: IEEE 19th International Workshop on Robotics in Alpe-Adria-Danube Region, RAAD, Budapest, Hungary, June 24–26, 2010, pp. 55–60, http://dx.doi.org/10.1109/RAAD.2010.5524609.
[186] T. Felzer, B. Freisleben, HaWCoS: the "hands-free" wheelchair control system, in: Proceedings of the 5th international Annual ACM Conference on Assistive Technologies, Edinburgh, UK, July 8–10, 2002, pp. 127–134, http://dx.doi.org/10.1145/638249.638273.
[187] Q. Sun, Y. Sun, X. Ding, Z. Ma, Onset determination of muscle contraction in surface electromyography signals analysis, in: ICIA 2005 – Proceedings of 2005 International Conference on Information Acquisition, June 27–July 3, 2005, pp. 384–387, http://dx.doi.org/10.1109/ICIA.2005.1635117.
[188] X. Zhang, X. Wang, B. Wang, T. Sugi, M. Nakamura, Finite state machine with adaptive electromyogram (EMG) feature extraction to drive meal assistance robot, IEEJ Trans. Electr. Inform. Syst. 129 (2) (2009) 308–313, http://dx.doi.org/10.1541/ieejeiss.129.308.
[189] L. Wei, H. Hu, EMG and visual based HMI for hands-free control of an intelligent wheelchair, in: Intelligent Control and Automation, July 7–9, 2010, pp. 1027–1032, http://dx.doi.org/10.1109/WCICA.2010.5554766.
[190] X. Zhang, X. Chen, W. Wang, J. Yang, V. Lantz, K. Wang, Hand gesture recognition and virtual game control based on 3D accelerometer and EMG sensors, in: IUI '09 Proceedings of the 14th International Conference on Intelligent User Interfaces, Sanibel Island, FL, USA, February 8–11, 2009, pp. 401–406, http://dx.doi.org/10.1145/1502650.1502708.
[191] A. Fougner, E. Scheme, A.D. Chan, K. Englehart, O. Stavdahl, Resolving the limb position effect in myoelectric pattern recognition, IEEE Trans. Neural Syst. Rehabil. Eng.: Publ. IEEE Eng. Med. Biol. Soc. 19 (6) (2011) 644–651, http://dx.doi.org/10.1109/TNSRE.2011.2163529.
[192] I. Moon, M. Lee, J. Ryu, M. Mun, Intelligent robotic wheelchair with EMG-, gesture-, and voice-based interfaces, in: IEEE/RSJ International Conference on Intelligent Robots and Systems, IROS 2003, October 27–31, 2003, pp. 3453–3458, http://dx.doi.org/10.1109/IROS.2003.1249690.
[193] M. Hashimoto, K. Takahashi, M. Shimada, Wheelchair control using an EOG- and EMG-based gesture interface, in: IEEE/ASME International Conference on Advanced Intelligent Mechatronics, AIM 2009, Singapore, July 14–17, 2009, pp. 1212–1217, http://dx.doi.org/10.1109/AIM.2009.5229752.
[194] A. Ferreira, R.L. Silva, W.C. Celeste, T.F. Filho, M.S. Filho, Human–machine interface based on muscular and brain signals applied to a robotic wheelchair, in: 16th Argentine Bioengineering Congress and the 5th Conference of Clinical Engineering, SABI 2007, vol. 90(1), September 26–28, 2007, pp. 1–8, http://dx.doi.org/10.1088/1742-6596/90/1/012094.
[195] X. Zhang, C. Xiang, L. Yun, V. Lantz, W. Kongqiao, Y. Jihai, A framework for hand gesture recognition based on accelerometer and EMG sensors, IEEE Trans. Syst. Man Cybern.: A 41 (6) (2011) 1064–1076, http://dx.doi.org/10.1109/TSMCA.2011.2116004.
[196] K. Davidge, Multifunction Myoelectric Control using a Linear Electrode Array (ProQuest Dissertation), University of New Brunswick, Canada, 2005.
[197] J.J. Baker, E. Scheme, K. Englehart, D.T. Hutchinson, B. Greger, Continuous detection and decoding of dexterous finger flexions with implantable myoelectric sensors, IEEE Trans. Rehabil. Eng. Neural Syst. 18 (4.) (2010) 424–432, http://dx.doi.org/10.1109/TNSRE.2010.2047590.
[198] A. Boschmann, M. Platzner, M. Robrecht, M. Hahn, M. Winkler, Development of a pattern recognition based myoelectric transhumeral prosthesis with multifunctional simultaneous control using a model-driven approach for mechatronic systems, in: Proceedings of the MyoElectric Controls/Powered Prosthetics Symposium Fredericton, New Brunswick, Canada, August 14–19, 2011.
[199] H. Rehbaum, N. Jiang, H. Rehbaum, A. Holobar, B. Graimann, H. Dietl, O.C. Aszmann, The extraction of neural information from the surface EMG for the control of upper-limb prostheses: emerging avenues and challenges, IEEE Trans. Neural Syst. Rehabil. Eng. 22 (4) (2014) 797–809, http://dx.doi.org/10.1109/TNSRE.2014.2305111.
[200] S. Muceli, N. Jiang, D. Farina, Multichannel surface EMG based estimation of bilateral hand kinematics during movements at multiple degrees of freedom, in: 32nd Annual International Conference of the IEEE Engineering in Medicine and Biology Society, EMBC, Buenos Aires, Argentina, September 1–4, 2010, pp. 6066–6069, http://dx.doi.org/10.1109/IEMBS.2010.5627622.
[201] J.L.G. Nielsen, S. Holmgaard, N. Jiang, K.B. Englehart, D. Farina, P.A. Parker, Simultaneous and proportional force estimation for multifunction myoelectric prostheses using mirrored bilateral training, IEEE Trans. Biomed. Eng. 58 (3) (2011) 681–688, http://dx.doi.org/10.1109/TBME.2010.2068298.
[202] S. Muceli, D. Farina, Simultaneous and proportional estimation of hand kinematics from EMG during mirrored movements at multiple degrees-of-freedom, IEEE Trans. Neural Syst. Rehabil. Eng. 20 (3) (2012) 371–378, http://dx.doi.org/10.1109/TNSRE.2011.2178039.
[203] N. Jiang, I. Vujaklija, H. Rehbaum, B. Graimann, D. Farina, Is accurate mapping of EMG signals on kinematics needed for precise online myoelectric

control? IEEE Trans. Neural Syst. Rehabil. Eng. 22 (3) (2014) 549–558, http://dx.doi.org/10.1109/TNSRE.2013.2287383.
[204] J.M. Hahne, F. Biessmann, N. Jiang, H. Rehbaum, D. Farina, F.C. Meinecke, K.-R. Muller, L.C. Parra, Linear and nonlinear regression techniques for simultaneous and proportional myoelectric control, IEEE Trans. Neural Syst. Rehabil. Eng. 22 (2) (2014) 269–279, http://dx.doi.org/10.1109/TNSRE.2014.2305520.
[205] E. Bizzi, P. Saltiel, A. D'avella, New perspectives on spinal motor systems, Nat. Rev. Neurosci. 1 (2) (2000) 101–108, http://dx.doi.org/10.1038/35039000.
[206] A. D'avella, E. Bizzi, Shared and specific muscle synergies in natural motor behaviors, Proceedings of the National Academy of Sciences of the United States of America 102 (February (8)) (2005) 3076–3081, http://dx.doi.org/10.1073/pnas.0500199102.
[207] N. Jiang, K.B. Englehart, P.A. Parker, Extracting simultaneous and proportional neural control information for multiple-DOF prostheses from the surface electromyographic signal, IEEE Trans. Biomed. Eng. 56 (4) (2009) 1070–1080, http://dx.doi.org/10.1109/TBME.2008.2007967.
[208] N. Jiang, H. Rehbaum, I. Vujaklija, B. Graimann, D. Farina, Intuitive, online, simultaneous, and proportional myoelectric control over two degrees-of-freedom in upper limb amputees, IEEE Trans. Neural Syst. Rehabil. Eng. 22 (3) (2014) 501–510, http://dx.doi.org/10.1109/TNSRE.2013.2278411.
[209] H. Rehbaum, N. Jiang, L. Paredes, S. Amsuess, B. Graimann, D. Farina, Real-time simultaneous and proportional control of multiple degrees of freedom from surface EMG: preliminary results on subjects with limb deficiency, in: 34th Annual International Conference of the IEEE Engineering in Medicine and Biology Society, EMBC, San Diego, CA, USA, August 28–September 1, 2012, pp. 1346–1349, http://dx.doi.org/10.1109/EMBC.2012.6346187.
[210] S. Muceli, N. Jiang, D. Farina, Extracting signals robust to electrode number and shift for online simultaneous and proportional myoelectric control by factorization algorithms, IEEE Trans. Neural Syst. Rehabil. Eng. 22 (3) (2014) 623–633, http://dx.doi.org/10.1109/TNSRE.2013.2282898.
[211] P.K. Artemiadis, K.J. Kyriakopoulos, EMG-based control of a robot arm using low-dimensional embeddings, IEEE Trans. Robot. 26 (2) (2010) 393–398, http://dx.doi.org/10.1109/TRO.2009.2039378.
[212] M.V. Liarokapis, P.K. Artemiadis, K.J. Kyriakopoulos, Task discrimination from myoelectric activity: a learning scheme for EMG-based interfaces, in: IEEE 13th International Conference on Rehabilitation Robotics, ICORR, Seattle, Washington, USA, June 24–26, 2013, pp. 1–6, http://dx.doi.org/10.1109/ICORR.2013.6650366.
[213] J.C. Jamison, G.E. Caldwell, Muscle synergies and isometric torque production: influence of supination and pronation level on elbow flexion, J. Neurophysiol. 70 (3) (1993) 947–960.
[214] D.T. Maclsaac, P.A. Parker, R.N. Scott, K.B. Englehart, C. Duffley, Influences of dynamic factors on myoelectric parameters, IEEE Eng. Med. Biol. Mag. 20 (6) (2001) 82–89, http://dx.doi.org/10.1109/51.982279.
[215] A. Al-Timemy, G. Bugmann, J. Escudero, N. Outram, A preliminary investigation of the effect of force variation for myoelectric control of hand prosthesis, in: 35th Annual International Conference of the IEEE Engineering in Medicine and Biology Society, EMBC, Osaka, Japan, July 3–7, 2013, pp. 5758–5761, http://dx.doi.org/10.1109/EMBC.2013.6610859.
[216] O. Fukuda, T. Tsuji, M. Kaneko, A. Otsuka, A human-assisting manipulator teleoperated by EMG signals and arm motions, IEEE Trans. Robot. Autom. 19 (2) (2003) 210–222, http://dx.doi.org/10.1109/TRA.2003.808873.
[217] R. Kato, H. Yokoi, T. Arai, Real-time learning method for adaptable motion-discrimination using surface EMG signal, in: IEEE/RSJ International Conference on Intelligent Robots and Systems, Beijing, China, October 9–15, 2006, pp. 2127–2132, http://dx.doi.org/10.1109/IROS.2006.282492.
[218] M. Hamedi, S.-H. Salleh, M. Astaraki, A.M. Noor, EMG-based facial gesture recognition through versatile elliptic basis function neural network, Biomed. Eng. Online 12 (73) (2013), http://dx.doi.org/10.1186/1475-925X-12-73.
[219] S. Jaiyen, C. Lursinsap, S. Phimoltares, A very fast neural learning for classification using only new incoming datum, IEEE Trans. Neural Netw. 21 (3) (2010) 381–392, http://dx.doi.org/10.1109/TNN.2009.2037148.
[220] M. Vuskovic, D. Sijiang, Classification of prehensile EMG patterns with simplified fuzzy ARTMAP networks, in: Proceedings of the 2002 International Joint Conference on Neural Networks, 2002. IJCNN '02, vol. 3, Honolulu, Hawaii, May 12–17, 2002, pp. 2539–2544, http://dx.doi.org/10.1109/IJCNN.2002.1007543.
[221] S. Herle, P. Raica, G. Lazea, R. Robotin, C. Marcu, L. Tamas, Classification of surface electromyographic signals for control of upper limb virtual prosthesis using time-domain features, in: IEEE International Conference on Automation, Quality and Testing, Robotics, AQTR 2008, vol. 3, Cluj-Napoca, Romania, May 22–25, 2008, pp. 160–165, http://dx.doi.org/10.1109/AQTR.2008.4588902.
[222] B. Karlik, M.O. Tokhi, M. Alci, A fuzzy clustering neural network architecture for multifunction upper-limb prosthesis, IEEE Trans. Biomed. Eng. 55 (11) (2003) 1255–1261, http://dx.doi.org/10.1109/TBME.2003.818469.
[223] G.R. Mcmillan, The technology and applications of biopotential-based control, in: RTO Lecture Series on Alternative Control Technologies: Human Factors Issues, Bretigny, France, 1–11 October, 1998, p. 7, (Chapter 7).
[224] J. Butterfass, M. Grebenstein, H. Liu, G. Hirzinger, DLR-Hand II: next generation of a dextrous robot hand, in: IEEE International Conference on Robotics and Automation, ICRA, vol. 1, 21–26 May, 2001, pp. 109–114, http://dx.doi.org/10.1109/ROBOT.2001.932538.
[225] J.-S. Han, D.H. Stefanov, K.-H. Park, H.-B. Lee, D.-J. Kim, W.-K. Song, J.-S. Kim, Z.Z. Bien, Development of an EMG-based powered wheelchair controller for users with high-level spinal cord injury, in: International Conference of Control, Automation and System, ICCAS, Jeju Island, Korea, 2001, pp. 503–506.
[226] J.-H. Song, J.-W. Jung, S.-W. Lee, Z. Bien, Robust EMG pattern recognition to muscular fatigue effect for powered wheelchair control, J. Intell. Fuzzy Syst. 20 (1–2) (2009) 3–12, http://dx.doi.org/10.1007/11925231_114.
[227] J.S. Han, Z.Z. Bien, D.J. Kim, H.E. Lee, J.S. Kim, Human–machine interface for wheelchair control with EMG and its evaluation, in: Proceedings of the 25th Annual International Conference IEEE Engineering in Medicine and Biology Society, vol. 2, Cancun, Mexico, September 17–21, 2003, pp. 1602–1605, http://dx.doi.org/10.1109/IEMBS.2003.1279672.
[228] M.A. Oskoei, H. Huosheng, Myoelectric-based virtual joystick applied to electric powered wheelchair, in: IEEE/RSJ International Conference on Intelligent Robots and Systems, IROS 2008, Nice, France, September 22–26, 2008, pp. 2374–2379, http://dx.doi.org/10.1109/IROS.2008.4650664.
[229] K.-H. Kim, H.K. Kim, J.-S. Kim, W. Son, S.-Y. Lee, A biosignal-based human interface controlling a power-wheelchair for people with motor disabilities, ETRI J. 28 (1) (2006) 111–114, http://dx.doi.org/10.4218/etrij.06.0205.0069.
[230] K. Choi, M. Sato, Y. Koike, A new, human-centered wheelchair system controlled by the EMG signal, in: International Joint Conference on Neural Networks, IJCNN, 2006, IJCNN '06, Vancouver, BC, 2006, pp. 4664–4671, http://dx.doi.org/10.1109/IJCNN.2006.247118.
[231] Y. Oonishi, O. Sehoon, Y. Hori, A new control method for power-assisted wheelchair based on the surface myoelectric signal, IEEE Trans. Ind. Electr. 57 (9) (2010) 3191–3196, http://dx.doi.org/10.1109/TIE.2010.2051931.
[232] D. Reddy, P.R. Kumar, V. Rajesh, SEMG-based human machine interface for controlling wheel chair by using ANN, in: International Conference on Control, Automation, Communication and Energy Conservation, INCACEC, Jun 4–6, Perundurai, Erode, India, 2009, ISBN 978-1-4244-4789-3, pp. 1–6.
[233] P. Nilas, P. Rani, N. Sarkar, An innovative high-level human–robot interaction for disabled persons, in: IEEE International Conference on Robotics and Automation, 2004, Proceedings, ICRA '04, vol. 3, New Orleans, LA, USA, April 26–May 1, 2004, pp. 2309–2314, http://dx.doi.org/10.1109/ROBOT.2004.1307406.
[234] J. Rosen, M.B. Fuchs, M. Arcan, Performances of hill-type and neural network muscle models - toward a myosignal-based exoskeleton, Comput. Biomed. Res. 32 (5) (1999) 415–439, http://dx.doi.org/10.1006/cbmr.1999.1524.
[235] E.E. Cavallaro, J. Rosen, J.C. Perry, S. Burns, Real-time myoprocessors for a neural controlled powered exoskeleton arm, IEEE Trans. Biomed. Eng. 53 (11) (2006) 2387–2396, http://dx.doi.org/10.1109/TBME.2006.880883.
[236] K. Kiguchi, S. Kariya, K. Watanabe, K. Izumi, T. Fukuda, An exoskeletal robot for human elbow motion support-sensor fusion, adaptation, and control, IEEE Trans. Syst. Man Cybern. B: Cybern. 31 (3) (2001) 353–361, http://dx.doi.org/10.1109/3477.931520.
[237] R. Song, K.Y. Tong, Using recurrent artificial neural network model to estimate voluntary elbow torque in dynamic situations, Med. Biol. Eng. Comput. 43 (4) (2005) 473–480, http://dx.doi.org/10.1007/BF02344728.
[238] C.D. Joshi, N.V. Thakor, Classification of gait phases from lower limb EMG: application to exoskeleton orthosis, in: IEEE Point-of-Care Healthcare Technologies (PHT), Bangalore, India, January 16–18, 2013, pp. 228–231, http://dx.doi.org/10.1109/PHT.2013.6461326.
[239] K.S. Kim, J.H. Kang, Y.H. Lee, C.S. Moon, H.H. Choi, C.W. Mun, The development of muscle training system using the electromyogram and interactive game for physical rehabilitation, in: 5th Kuala Lumpur International Conference on Biomedical Engineering 2011, IFMBE Proceedings, vol. 35, Kuala Lumpur, Malaysia, June 20–23, 2011, pp. 801–804, http://dx.doi.org/10.1007/978-3-642-21729-6_196.
[240] G.M. Lyons, P. Sharma, M. Baker, S. O'malley, A. shanahan, A computer game-based EMG biofeedback system for muscle rehabilitation, in: Proceedings of the 25th Annual International Conference of the IEEE Engineering in Medicine and Biology Society, EMBC, vol. 2, August 31–September 4, 2003, pp. 1625–1628, http://dx.doi.org/10.1109/IEMBS.2003.1279682.
[241] N.S. Ho, K.Y. Tong, X.L. Hu, K.L. Fung, X.J. Wei, W. Rong, E.A. Susanto, An EMG-driven exoskeleton hand robotic training device on chronic stroke subjects: task training system for stroke rehabilitation, in: IEEE International Conference on Rehabilitation Robotics, ICORR, Zurich, Switzerland, June 29–July 1, 2011, pp. 1–5, http://dx.doi.org/10.1109/ICORR.2011.5975340.
[242] T. Lenzi, S.M. De Rossi, N. Vitiello, M.C. Carrozza, Intention-based EMG control for powered exoskeletons, IEEE Trans. Biomed. Eng. 59 (8) (2012) 2180–2190, http://dx.doi.org/10.1109/TBME.2012.2198821.
[243] K. Kiguchi, Y. Imada, M. Liyanage, EMG-based neuro-fuzzy control of a 4dof upper-limb power-assist exoskeleton, in: 29th Annual International Conference of the IEEE Engineering in Medicine and Biology Society, EMBC, Lyon, France, August 23–26, 2007, pp. 3040–3043, http://dx.doi.org/10.1109/IEMBS.2007.4352969.
[244] S.E. Hussein, M.H. Granat, Intention detection using a neuro-fuzzy EMG classifier, IEEE Eng. Med. Biol. Mag. 21 (November/December (6)) (2002) 123–129, http://dx.doi.org/10.1109/MEMB.2002.1175148.
[245] K. Kiguchi, Q. Qilong, Muscle-model-oriented EMG-based control of an upper-limb power-assist exoskeleton with a neuro-fuzzy modifier, in: IEEE International Conference on Fuzzy Systems, FUZZ-IEEE 2008 (IEEE World Congress on Computational Intelligence), Hong Kong, June 1–6, 2008, pp. 1179–1184, http://dx.doi.org/10.1109/FUZZY.2008.4630520.
[246] Y.J. Fan, Z. Guo, Y. Yin, SEMG-based neuro-fuzzy controller for a parallel ankle exoskeleton with proprioception, Int. J. Robot. Autom. 26 (4) (2011) 450–460, http://dx.doi.org/10.2316/Journal.206.2011.4.206-3590.

[247] R.A.R.C. Gopura, K. Kiguchi, A human forearm and wrist motion assist exoskeleton robot with EMG-based fuzzy-neuro control, in: 2nd IEEE RAS & EMBS International Conference on Biomedical Robotics and Biomechatronics, BioRob 2008, Oct. 19-22, Scottsdale, AZ, 2008, pp. 550–555, http://dx.doi.org/10.1109/BIOROB.2008.4762793.

[248] K. Kiguchi, M.H. Rahman, M. Sasaki, Neuro-fuzzy based motion control of a robotic exoskeleton: considering end-effector force vectors, in: Proceedings 2006 IEEE International Conference on Robotics and Automation, ICRA 2006, May 15–19, Orlando, FL, USA, 2006, pp. 3146–3151, http://dx.doi.org/10.1109/ROBOT.2006.1642180.

[249] A. Xiong, Y. Chen, X. Zhao, J. Han, G. Liu, A novel HCI-based on EMG and IMU, in: IEEE International Conference on Robotics and Biomimetics, ROBIO, Karon Beach, Phuket, Thailand, December 7–11, 2011, pp. 2653–2657, http://dx.doi.org/10.1109/ROBIO.2011.6181705.

[250] K.R. Wheeler, C.C. Jorgensen, Gestures as input: neuroelectric joysticks and keyboards, IEEE Pervas. Comput. 2 (2) (2003) 56–61, http://dx.doi.org/10.1109/MPRV.2003.1203754.

[251] H. Benko, S. Saponas, D. Morris, D. Tan, Enhancing input on and above the interactive surface with muscle sensing. Interactive tabletops and surfaces, in: Proceedings of the ACM International Conference, ITS '09, Karon Beach, Phuket, Thailand, December 7–11, 2009, pp. 93–100, http://dx.doi.org/10.1145/1731903.1731924.

[252] D.G. Park, H.C. Kim, Muscleman: Wireless Input Device for a Fighting Action Game based on the EMG Signal and Acceleration of the Human Forearm, web publication, Available from: http://www.intuinno.com/uploads/1/0/2/9/10297987/muscleman_paper.pdf. More information related to the reference 252 can be found in http://www.intuinno.com/muscleman.html

[253] A.D.C. Chan, K. Englehart, B. Hudgins, D.F. Lovely, Myo-electric signals to augment speech recognition, Med. Biol. Eng. Comput. 39 (4) (2001) 500–504, http://dx.doi.org/10.1007/BF02345373.

[254] M.S. Morse, S.H. Day, B. Trull, H. Morse, Use of myoelectric signals to recognize speech, in: Engineering in Medicine and Biology Society, 1989. Proceedings of the Annual International Conference of the IEEE Engineering in Images of the Twenty-First Century, vol. 6, Seattle, WA, USA, November 9–12, 1989, pp. 1793–1794, http://dx.doi.org/10.1109/IEMBS.1989.96459.

[255] C.C. Jorgensen, D.D. Lee, S. Agabont, Sub-auditory speech recognition based on EMG signals, in: Proceedings of the International Joint Conference on Neural Networks, IJCNN, vol. 4, July 20–21, 2003, pp. 3128–3133, http://dx.doi.org/10.1109/IJCNN.2003.1224072.

[256] B.J. Betts, C. Jorgensen, Small Vocabulary Recognition using Surface Electromyography in an Acoustically Harsh Environment, Sponsoring Organization: NASA Ames Research Center|QSS Group, Inc., 2005, Available from: http://ntrs.nasa.gov/archive/nasa/casi.ntrs.nasa.gov/20050242013.pdf

[257] M.S. Morse, Y.N. Gopalan, M. Wright, Speech recognition using myoelectric signals with neural networks, in: Proceedings of the Annual International Conference of the IEEE Engineering in Medicine and Biology Society, vol. 13, October 31–November 3, 1991, pp. 1877–1878, http://dx.doi.org/10.1109/IEMBS.1991.684800.

[258] M. Wand, S-C.S. Jou, A.R. Toth, T. Schultz, Impact of different speaking modes on EMG-based speech recognition, in: Proceedings of the Annual Conference of the International Speech Communication Association, ISCA, INTERSPEECH 2009, Brighton, UK, September 6–10, 2009, pp. 648–651, ISSN: 19909772.

[259] E.J. Scheme, B. Hudgins, P.A. Parker, Myoelectric signal classification for phoneme-based speech recognition, IEEE Trans. Biomed. Eng. 54 (4) (2007) 694–699, http://dx.doi.org/10.1109/TBME.2006.889175.

[260] Q. Zhou, N. Jiang, K. Englehart, B. Hudgins, Improved phoneme-based myoelectric speech recognition, IEEE Trans. Biomed. Eng. 56 (8) (2009) 2016–2023, http://dx.doi.org/10.1109/TBME.2009.2024079.